JCB

Article

Src-mediated phosphorylation converts FHL1 from tumor suppressor to tumor promoter

Xiang Wang,[1]* Xiaofan Wei,[1]* Yang Yuan,[1] Qingrui Sun,[1] Jun Zhan,[1] Jing Zhang,[1] Yan Tang,[1] Feng Li,[1] Lihua Ding,[2] Qinong Ye,[2] and Hongquan Zhang[1]

[1]Key Laboratory of Carcinogenesis and Translational Research (Ministry of Education), Department of Human Anatomy, Histology and Embryology, and State Key Laboratory of Natural and Biomimetic Drugs, Peking University Health Science Center, Beijing, China
[2]Department of Medical Molecular Biology, Beijing Institute of Biotechnology, Collaborative Innovation Center for Cancer Medicine, Beijing, China

FHL1 has been recognized for a long time as a tumor suppressor protein that associates with both the actin cytoskeleton and the transcriptional machinery. We present in this study a paradigm that phosphorylated FHL1 functions as an oncogenic protein by promoting tumor cell proliferation. The cytosolic tyrosine kinase Src interacts with and phosphorylates FHL1 at Y149 and Y272, which switches FHL1 from a tumor suppressor to a cell growth accelerator. Phosphorylated FHL1 translocates into the nucleus, where it binds to the transcription factor BCLAF1 and promotes tumor cell growth. Importantly, the phosphorylation of FHL1 is increased in tissues from lung adenocarcinoma patients despite the down-regulation of total FHL1 expression. Kindlin-2 was found to interact with FHL1 and recruit FHL1 to focal adhesions. Kindlin-2 competes with Src for binding to FHL1 and suppresses Src-mediated FHL1 phosphorylation. Collectively, we demonstrate that FHL1 can either suppress or promote tumor cell growth depending on the status of the sites for phosphorylation by Src.

Introduction

Four-and-a-half LIM (FHL) protein 1 (FHL1) belongs to the FHL protein family, which consists of four members, FHL1, FHL2, FHL3, and FHL5 in humans. All these proteins are characterized by the tandem arrangement of four and a half highly conserved LIM domains. LIM domains mediate protein–protein interactions and are involved in linking proteins with both the actin cytoskeleton and the transcriptional machinery (Kadrmas and Beckerle, 2004; Shathasivam et al., 2010). FHL1 is highly expressed in skeletal muscle and heart (Greene et al., 1999) and has been associated with skeletal muscle myopathies and several cardiovascular diseases (Cowling et al., 2008; Willis et al., 2016). Interestingly, FHL1 is markedly down-regulated in a variety of cancers including lung (Niu et al., 2012), liver (Ding et al., 2009), breast (Ding et al., 2011), colon, renal (Li et al., 2008), and gastric cancers (Xu et al., 2012). FHL1 was previously identified as a tumor suppressor protein, which acts to inhibit tumor cell growth and migration. Recently, our study (Xu et al., 2017) showed that FHL1 leads to radiation resistance in cancer cells by inhibiting CDC25C activity. Moreover, increased expression of FHL1 led to significantly poorer disease-free survival and overall survival rates for breast cancer patients who received radiotherapy, indicating that the role and mechanism of FHL1 in cancer progression is more complex and diverse than was previously thought. Whether FHL1 is an implicit tumor cell growth suppressor needs to be questioned and investigated. Additionally, although it is certain that FHL1 expression is down-regulated in many cancers, the posttranslational modification of FHL1 and the potential role of such modifications in cancer progression remain unclear.

Previous research has indicated that FHL1 localizes to the nucleus and focal adhesions via integrin activation, where it then functions to promote cell spreading and migration (Robinson et al., 2003). Upon activation, integrins subsequently activate cytoplasmic kinases and cytoskeletal signaling cascades including enzymes (e.g., focal adhesion kinase [FAK], Src, and Rho GTPases) and adapters (e.g., paxillin; Guo and Giancotti, 2004; Harburger and Calderwood, 2009). With respect to FHL1, the components of the integrin-dependent signaling pathways that are responsible for FHL1 localization to the nucleus and focal adhesions and the functions of FHL1 at these specific locations remain unclear. Kindlin-2, a member of the kindlin protein family, is considered as an essential regulator of integrin activation and integrin-mediated cell–ECM adhesion (Larjava et al., 2008; Ma et al., 2008). Kindlin-2 is reported to act as an adapter protein, and as an important member of focal adhesion proteins, it interacts with and recruits migfilin (a LIM-containing protein) to cell–matrix adhesions and participates in the orchestration of actin assembly. Thus, we hypothesize that FHL1 is recruited to focal adhesions by interacting with kindlin-2.

*X. Wang and X. Wei contributed equally to this paper.

Correspondence to Hongquan Zhang: Hongquan.Zhang@bjmu.edu.cn

The Rockefeller University Press
J. Cell Biol. Vol. 217 No. 4 1335–1351
https://doi.org/10.1083/jcb.201708064

The cellular Src tyrosine kinases are the first molecules to be recruited to focal adhesions after the activation of integrins (Guo and Giancotti, 2004). Src, a nonreceptor tyrosine kinase, was confirmed as a critical component of a variety of pathways that regulate important cellular functions including proliferation, survival, adhesion, and migration (Yeatman, 2004). Importantly, Src is up-regulated, highly activated, and believed to play a pivotal role in numerous types of human cancers (Ishizawar and Parsons, 2004; Guarino, 2010). However, the molecular mechanism underlying Src-mediated tumor progression remains elusive. In this study, we demonstrate that Src interacts with and induces phosphorylation of FHL1. Upon phosphorylation, FHL1 translocates into the nucleus and promotes tumor cell growth by cooperating with transcription factor BCLAF1, which changes the role of FHL1 from a tumor suppressor to a tumor promoter. Interestingly, FHL1 can be recruited to focal adhesions by interaction with kindlin-2, and then kindlin-2 competes with Src in binding to FHL1. Excessive kindlin-2 mediates the stable localization of FHL1 at focal adhesions to function downstream of integrin activation.

Results

FHL1 interacts with Src in vivo and in vitro

FHL1 is known to be involved in integrin-mediated signaling pathways and regulates functions with the cytosolic tyrosine kinases Src and FAK (Mitra and Schlaepfer, 2006). We hypothesized that there may be some interplay between FHL1 and Src and FAK. To this end, Flag-FHL1 and HA-Src were transfected into HeLa cells, and then coimmunoprecipitations (co-IPs) were performed (Fig. 1, A and B). These results show that exogenous FHL1 physically interacts with exogenous Src (Fig. 1, A and B). Furthermore, endogenous FHL1 and endogenous Src also showed a strong association in a co-IP assay (Fig. 1, C and D). However, a potential interaction between FHL1 and FAK could not be detected (Fig. 1 C). We thus focused on the FHL1 and Src interaction and its biological consequence. To determine whether this is a direct interaction, both full-length His-FHL1 and GST-Src or GST-FHL1 proteins were expressed and purified from *Escherichia coli*, and then GST/His pulldown assays were performed. These results show that purified FHL1 strongly interacted with Src (Fig. 1, E and F). Consistently, FHL1 was found to be colocalized with Src mainly at focal adhesion sites in HeLa cells as indicated by immunofluorescence staining (Fig. 1 G). Collectively, these data demonstrate a previously unknown molecular interaction between FHL1 and Src both in vivo and in vitro.

To define which regions of FHL1 and Src were responsible for mediating their interaction, truncated constructs of FHL1 and Src were made according to their functional domains (Fig. 1, H and I; Cowling et al., 2011; Roskoski, 2015). GST pulldown analyses showed that the mutants of FHL1 (aa 56–280 and aa 117–280) contained a LIM4 domain associated with Src (Fig. 1 J), whereas other mutants could not bind to Src. This indicates that the last LIM domain of FHL1 mediates its interaction with Src. Furthermore, we found that the kinase domain of Src mediates its interaction with FHL1 (Fig. 1 K). Collectively, these results clearly indicate that the LIM4 domain of FHL1 interacts with the kinase domain of Src.

Src phosphorylates FHL1 at aa Y149 and Y272

It is well known that Src phosphorylates tyrosine residues, which regulate numerous cellular processes including cell proliferation, migration, and differentiation (Yeatman, 2004). The aforementioned interaction between FHL1 and Src suggests that Src may phosphorylate FHL1. However, thus far, there are no known FHL1 posttranslational modifications. We therefore attempted to determine whether Src is able to phosphorylate FHL1. To this end, HeLa cells were cotransfected with Flag-FHL1 and HA-tagged WT Src (Src-WT), Src kinase-dead (KD) variant (Src-KD), or constitutively activated (CA) Src (Src-CA). Cell lysates containing FHL1 were harvested, and a co-IP was performed with anti-Flag M2 beads. Tyrosine-phosphorylated FHL1 was detected with an antiphosphotyrosine antibody (PY20). Results in Fig. 2 A show that Src-WT markedly induced tyrosine phosphorylation on FHL1 without affecting FHL1 expression levels and that Src-CA dramatically increased FHL1 phosphorylation compared with that of Src-WT. Kindlin-2 phosphorylation was used as a positive control as previous studies have already demonstrated that Src could phosphorylate kindlin-2 (Qu et al., 2014; Liu et al., 2015). Moreover, Src-induced FHL1 phosphorylation occurred in a dose-dependent manner (Fig. 2 B). Importantly, Src-KD did not show phosphorylation on FHL1 (Fig. 2, A and B), suggesting that FHL1 phosphorylation is dependent on Src kinase activity. To further confirm that Src could phosphorylate FHL1, an in vitro phosphorylation assay was performed. Indeed, using purified proteins, we showed that Src could phosphorylate FHL1 on tyrosine in vitro and that the phosphorylation is in a dose-dependent manner (Fig. 2, C and D). Furthermore, to examine the specificity of this Src-mediated phosphorylation, λ protein phosphatase (λ-phosphatase) was applied, and these results indicate that this phosphatase effectively inhibited Src-induced FHL1 phosphorylation (Fig. 2 E). In addition, treatment of HeLa cells with PP2 (a specific inhibitor of the Src family kinases) for 12 h resulted in reduced tyrosine phosphorylation of exogenous FHL1 in a dose-dependent manner (Fig. 2 F). We then examined the protein level of Src in HeLa and H1299 cells, and the results show that both Src and p-Src were highly expressed in H1299 cells as compared with HeLa cells (Fig. 2 G). Therefore, H1299 cells were used to determine the role of Src in the phosphorylation of endogenous FHL1. The results showed that phosphorylation of endogenous FHL1 in H1299 cells decreased significantly after PP2 treatment (Fig. 2 H).

To identify the Src-associated FHL1 phosphorylation sites, mass spectrometry was performed on FHL1 proteins isolated from HeLa cells. Data showed that the potential phosphorylation sites are located at Y117, Y149, Y213, and Y272 of FHL1 (Fig. S1, A–C). To validate the mass spectrometry findings, four FHL1 mutants with Y-to-F mutation were generated, and phosphorylation assays were performed in vivo. Among the four FHL1 mutants, we found that mutants Y149F and Y272F mostly lost the ability to be phosphorylated by Src (Fig. 2 I), indicating that Y149 and Y272 are the sites within FHL1 that can be phosphorylated by Src in vivo. To examine whether the identified phosphorylated sites exist in living cells, we produced phosphospecific antibodies recognizing phosphorylated FHL1 at tyrosines 149 and 272. As shown in Fig. 2 (J and K), Src-induced phosphorylation of FHL1 could be detected by the anti–p-Y149 and –p-Y272 antibodies, but phosphorylation of FHL1-Y149F and -Y272F

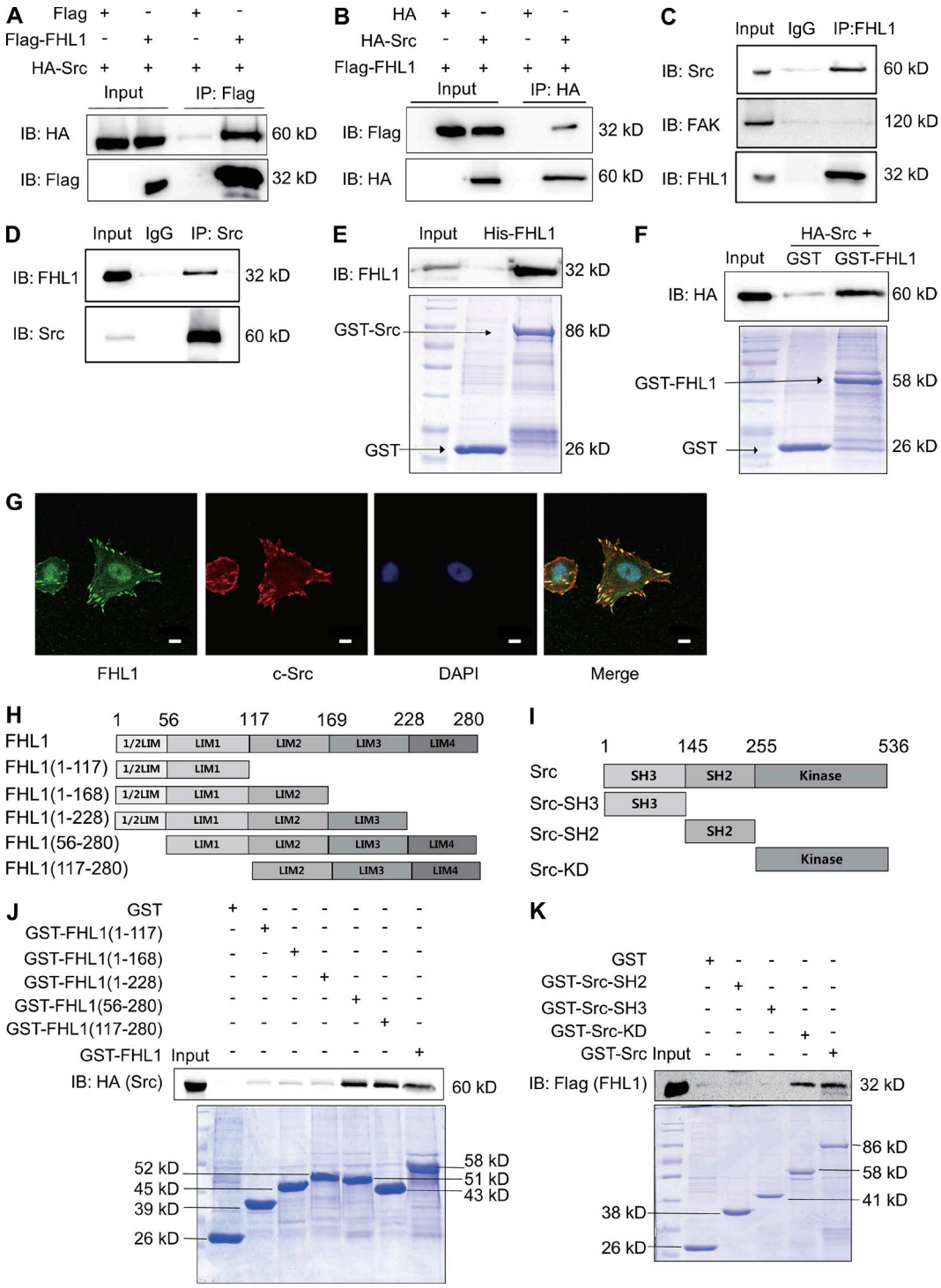

Figure 1. **FHL1 interacts with Src in vivo and in vitro. (A)** HeLa cells were transfected with indicated plasmids. 48 h after transfection, cell lysates were immunoprecipitated with anti-Flag M2 beads followed by immunoblotting (IB) using HA antibody. **(B)** HeLa cells were transfected with indicated plasmids. 48 h after transfection, cell lysates were immunoprecipitated with anti-HA antibody followed by immunoblotting using Flag antibody. **(C and D)** The endogenous interaction between FHL1 and Src was analyzed by co-IP. Co-IP assays were performed using lysates from H1299 cells with control IgG or anti-FHL1 antibody followed by immunoblotting with anti-Src and anti-FAK antibody (C). H1299 cells were lysed, and equal amounts of protein lysates were immunoprecipitated with anti-Src antibody or IgG and probed with anti-FHL1 antibody (D). **(E)** Fusion protein His-FHL1 was incubated with GST or GST-Src in vitro for GST pulldown assays. **(F)** Purified GST-FHL1 or GST protein was incubated with H1299 cell lysates at 4°C overnight. Beads were washed, and the remaining proteins were resolved by SDS-PAGE and further analyzed by Western blotting using anti-HA antibody. **(G)** Visualization of endogenous FHL1 and endogenous Src in HeLa cells. FHL1 (green) was colocalized with Src (red) in focal adhesion sites and cytoplasm. Bars, 10 μm. **(H and I)** Indicated truncates of FHL1 and Src were constructed according to their functional domains. **(J)** GST pulldown assays were performed using HeLa cells lysates transfected with HA-Src expression vector. GST-FHL1 fragments were purified using Glutathione Sepharose 4B beads, and then the beads were incubated with HeLa cell lysate at 4°C overnight. Src was analyzed by Western blotting using anti-HA antibody. **(K)** GST pulldown assays were performed using HeLa cells lysates transfected with Flag-FHL1 expression vector. GST-Src fragments were purified using Glutathione Sepharose 4B beads, and then beads were incubated with HeLa cell lysate at 4°C overnight. FHL1 was analyzed by Western blotting using anti-Flag antibody.

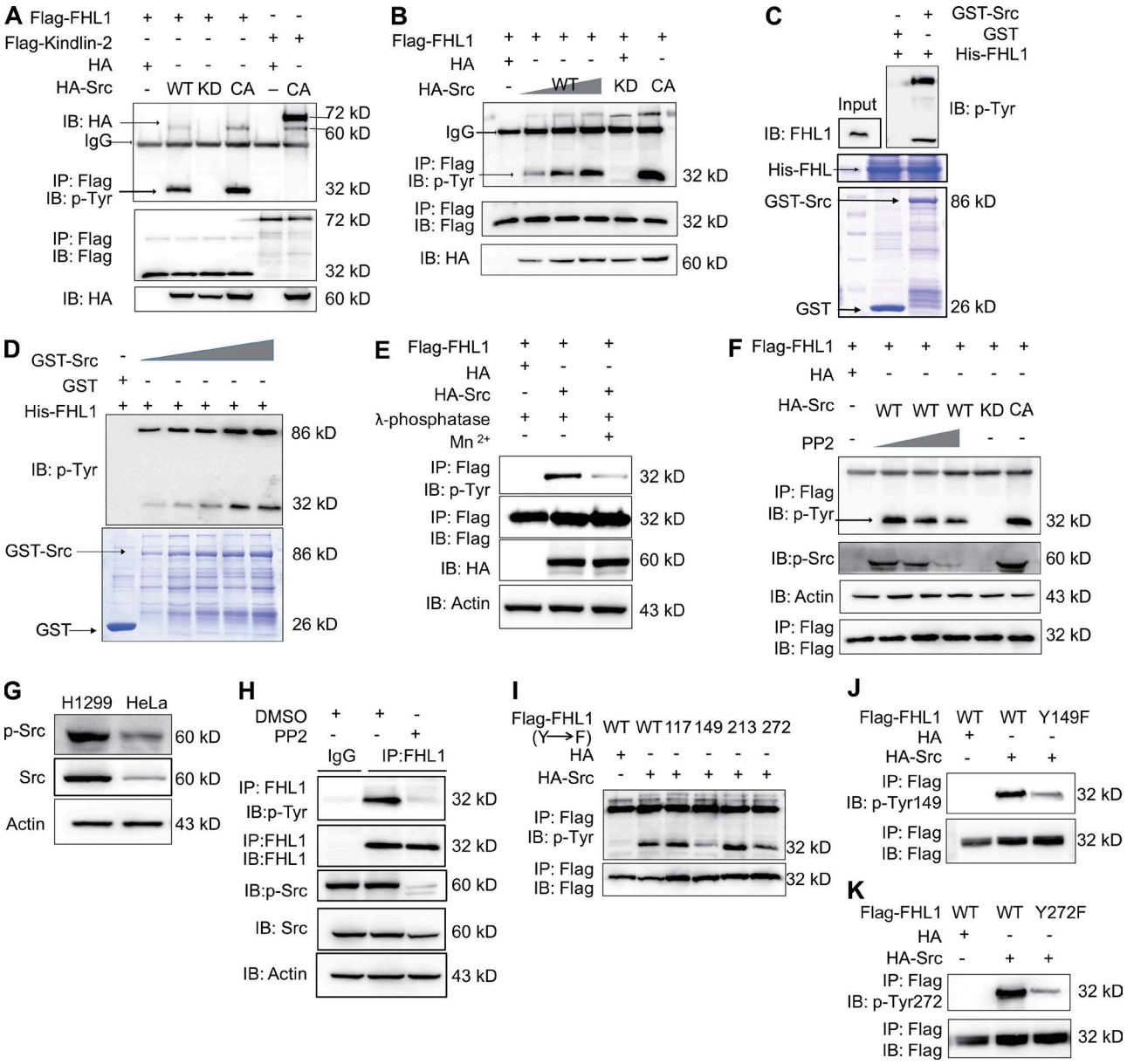

Figure 2. **Src phosphorylates FHL1 at Y149 and Y272. (A)** HeLa cells were transfected with indicated plasmids. 48 h after transfection, cell lysates were immunoprecipitated with anti-Flag M2 beads followed by immunoblotting (IB) using p-Tyr–100 antibody or anti-Flag or anti-HA antibody. Kindlin-2 was used as a positive control. **(B)** Flag-FHL1 plasmid was transfected into HeLa cells together with Src-KD or Src-CA or increasing amounts of WT Src plasmid. Immunoblots were probed with anti-Flag antibodies or the p-Tyr–100 antibody to show tyrosine phosphorylation of FHL1. **(C)** Src-phosphorylated FHL1 in vitro. In vitro phosphorylation assays were performed by using GST, GST-Src, and His-FHL1. Then, the reaction mixtures were subjected to SDS-PAGE followed by immunoblotting with the p-Tyr–100 antibody and FHL1 antibody. The purified His- and GST-tagged fusion proteins were stained by Coomassie blue. **(D)** Purified His-FHL1 protein was incubated with GST or increasing amounts GST-Src at 37°C for 30 min in kinase buffer, and in vitro phosphorylation assays were performed. **(E)** HeLa cells were transfected with indicated plasmids. Flag-FHL1 was immunoprecipitated by anti-Flag M2 beads. Then, IPs were treated with λ-phosphatase (with or without Mn^{2+}) for 60 min at 30°C and immunoblotted for p-Tyr and anti-Flag. **(F)** HeLa cells were transfected with indicated plasmids. Flag-FHL1 was immunoprecipitated from HeLa extracts after treatment with DMSO or increasing amounts of PP2 for 12 h and then immunoblotted for p-Tyr and Flag. **(G)** The expression of p-Src and Src in H1299 and HeLa cells were analyzed. **(H)** FHL1 was immunoprecipitated from H1299 extracts after treatment with 10 µM PP2 or DMSO for 12 h and immunoblotted with the p-Tyr–100 antibody. **(I)** Flag-tagged FHL1-WT or various FHL1 mutants (Y117F, Y149F, Y213F, and Y272F) were cotransfected with HA or HA–Src-WT in HeLa cells. After IP with anti-Flag M2 beads, FHL1 phosphorylation was detected by Western blot analysis with p-Tyr–100 and anti-Flag antibodies. **(J and K)** HeLa cells were transfected with Flag–FHL1-WT, FHL1-Y149F, or FHL1-Y272F mutant expression vectors together with HA or HA–Src-WT. Cell lysates were immunoprecipitated with anti-Flag M2 beads or immunoblotted with anti–p-Tyr149–FHL1 antibody or anti–p-Tyr272–FHL1 antibody.

mutants were hardly observed. Collectively, these in vitro and in vivo data demonstrate that FHL1 is a previously unrecognized substrate for Src, which phosphorylated FHL1 at Y149 and Y272. We demonstrated that FHL1 could be modulated by posttranslational modifications.

FHL1 interacts with kindlin-2 in vivo and in vitro

A previous study indicated that FHL1 localizes to nuclei and focal adhesions via integrin activation (Liu et al., 2015). An integrin-interacting focal adhesion molecule, kindlin-2, is known to

recruit the LIM domain–containing protein migfilin to focal adhesions, implying that kindlin-2 may also interact with other LIM domain–containing proteins. FHL1 is a LIM domain–containing protein consisting of four complete LIM domains arranged in tandem and an N-terminal single zinc finger domain with a consensus sequence equivalent to the C-terminal half of a LIM motif (Cowling et al., 2011). We therefore attempted to examine whether kindlin-2 may also physically interact with FHL1. To this end, Flag or Flag-FHL1 together with GFP–kindlin-2 were cotransfected into HeLa cells, and then a co-IP using anti-Flag M2 beads was performed. As shown in Fig. 3 A, Flag-FHL1 was found to interact with GFP–kindlin-2. Furthermore, endogenous kindlin-2 and FHL1 showed a strong association in a co-IP assay (Fig. 3, B and C). To test whether this interaction is direct, both full-length His–kindlin-2 and GST-FHL1 fusion proteins were expressed and purified from *E. coli*, and then GST pulldown assays were performed. The results showed that purified kindlin-2 interacted strongly with purified FHL1 (Fig. 3 D). Moreover, endogenous kindlin-2 was found to be colocalized with endogenous FHL1 mainly at focal adhesion sites in HeLa cells as determined by immunofluorescent staining (Fig. 3 E). To map the binding regions between kindlin-2 and FHL1, three truncated constructs of kindlin-2 were made (Fig. 3 F; Wei et al., 2017). Kindlin-2 consists of an N-terminal domain, a FERM domain in the middle region, and a C-terminal domain. As shown in Fig. 3 G, only the FERM domain of kindlin-2 interacted with FHL1, whereas both the N-terminal and C-terminal domains of kindlin-2 were unable to associate with FHL1 in a GST pulldown assay. Furthermore, as shown in Fig. 3 H, the mutants of FHL1 (aa 56–280 and aa 117–280) containing the LIM4 domain interacted with kindlin-2, whereas other mutants could not bind to FHL1. These data indicate that the last LIM domain of FHL1 is responsible for its interaction with kindlin-2, which is the same domain that mediates the interaction between FHL1 and Src. Collectively, these data demonstrate a previously unknown molecular interaction between kindlin-2 and FHL1 both in vivo and in vitro.

Src and kindlin-2 compete with each other in binding to FHL1

Given that both Src and kindlin-2 selectively interacted with the last LIM domain of FHL1, a competition for FHL1 binding may exist between Src and kindlin-2. To test this possibility, Src was overexpressed in HeLa cells, and the results showed that overexpression of Src weakened the exogenous interaction between FHL1 and kindlin-2 (Fig. 4 A). Moreover, the endogenous interaction between FHL1 and kindlin-2 was strengthened when Src activity was inhibited by PP2 in H1299 cells (Fig. 4 B). In addition, when kindlin-2 was overexpressed or depleted by siRNA, the interaction between FHL1 and Src was inhibited or enhanced, respectively (Fig. 4, C and D). Similarly, overexpression and knockdown of kindlin-2 suppressed and increased the Src-dependent phosphorylation of FHL1, respectively (Fig. 4, C–E). The intensity of the p-Tyr band from the FHL1 immunoprecipitation (IP) from three separate biological replicates in Fig. 4 (D and E) has been quantified and statistically analyzed and is shown in Fig. S2 (A and B). Importantly, the phosphomimetic mutant FHL1-Y149-272D mostly lost its ability to interact with kindlin-2 (Fig. 4 F). Collectively, these data indicate that kindlin-2 competes with Src to interact with FHL1. However, previous research and our data from this study all suggest that FHL1, Src, and kindlin-2 can be localized at focal adhesions (Brown et al., 1999; Guo and Giancotti, 2004). Given that kindlin-2 could function as a scaffold molecule in focal adhesions (Tu et al., 2003; Lai-Cheong et al., 2010), we thus aimed to examine the possibility that the endogenous proteins FHL1, Src, and kindlin-2 may form a tripartite molecular complex. To this end, reciprocal co-IP assays were performed. The results showed that the three molecules did form a complex (Fig. 4, G–I), and the interaction between FHL1, Src, and kindlin-2 was enhanced upon cell–ECM adhesion. In addition, immunofluorescent staining confirmed that endogenous FHL1, kindlin-2, and endogenous Src were mainly colocalized to focal adhesions upon cell–ECM adhesion and cell spreading processes (Fig. 4 J). Collectively, these findings indicate that FHL1, Src, and kindlin-2 are able to form a molecular complex upon cell–ECM adhesion; nevertheless, the fact that kindlin-2 competes with Src in interacting with FHL1 might determine the localization of FHL1 in cells.

Kindlin-2 is indispensable for FHL1 localization to the focal adhesions

The findings that FHL1 interacts with kindlin-2 and colocalizes to focal adhesions prompted us to test our hypothesis that FHL1 is recruited to focal adhesions by its interaction with kindlin-2, resembling the effect of kindlin-2 on migfilin. For this purpose, kindlin-2 was knocked down in HeLa cells, and the localization of FHL1 was visualized by immunofluorescent staining. Knockdown of kindlin-2 led to diffuse localization of FHL1 in the cytoplasm and nucleus, and FHL1 failed to cluster at focal adhesions (Fig. 5 A). To further confirm this localization, WT mouse embryonic fibroblast (MEF) cells and kindlin-2$^{+/-}$ MEF cells were applied, and cells were replated on fibronectin (FN) for 4 h. FHL1 and paxillin (as a marker of focal adhesions) were stained after cells were fully spread, and kindlin-2 depletion was confirmed by Western blot analysis (Fig. 5 B). As expected, clusters of paxillin were detected at cell–ECM adhesions in cells of both groups (Fig. 5 C). FHL1 in WT MEF cells showed a well-defined focal adhesion localization; however, FHL1 was localized diffusely in the cytoplasm and did not cluster at focal adhesions in the kindlin-2$^{+/-}$ MEF cells (Fig. 5 C). Similarly, knockdown of kindlin-2 in H1299 cells inhibited FHL1 localization to focal adhesions (Fig. S2 C). These data indicate that kindlin-2 is required for FHL1 localization to the focal adhesions.

Src promotes the nuclear translocation of FHL1

Although previous studies have suggested that FHL1 could localize to the nucleus and focal adhesions via integrin activation (Brown et al., 1999; Robinson et al., 2003), the molecular mechanisms underlying FHL1 subcellular localization remained elusive. Given that phosphorylation can alter the subcellular localization of proteins, we wondered whether FHL1 phosphorylation by Src might alter the localization of FHL1. To this end, immunofluorescent staining was applied, and the results showed that Flag–FHL1-WT was mainly localized to the cytoplasm. However, overexpression of Src promoted most of the Flag–FHL1-WT to translocate to the nucleus, whereas the Flag–FHL1-Y149-272F mutant (phosphorylation-deficient mutant) remained in the cytoplasm (Fig. 5 D). In agreement, cell fractionation analysis also demonstrated that Src promoted the nuclear translocation of both exogenous and endogenous FHL1-WT (Fig. 5, E and F). In contrast, the FHL1-Y149-272F mutant was unable to translocate into the nucleus (Fig. 5 E).

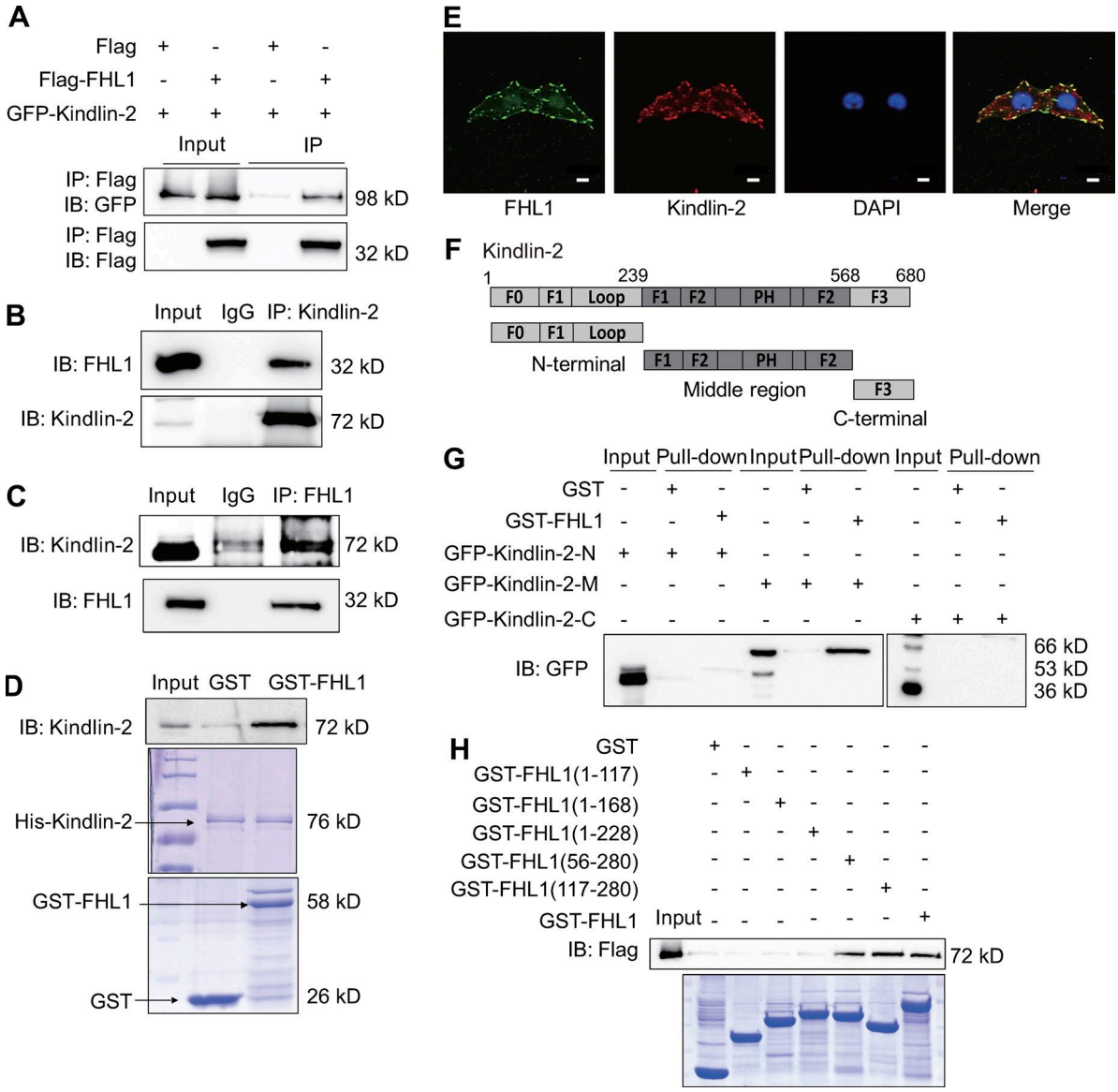

Figure 3. **FHL1 interacts with kindlin-2 in vivo and in vitro. (A)** HeLa cells were transfected with indicated plasmids. 48 h after transfection, cell lysates were immunoprecipitated with anti-Flag M2 beads followed by immunoblotting (IB) using GFP antibody. **(B and C)** The endogenous interaction between FHL1 and kindlin-2 was analyzed by co-IP. Co-IP assays were performed using lysates from H1299 cells with control IgG or anti–kindlin-2 antibody followed by immunoblotting with anti-FHL1 (B). H1299 cells were lysed, and equal amounts of protein lysates were immunoprecipitated with anti-FHL1 antibody or IgG and probed with anti–kindlin-2 antibody (C). **(D)** Fusion protein His–kindlin-2 was incubated with GST or GST-FHL1 in vitro for GST pulldown assays. **(E)** Visualization of endogenous FHL1 and endogenous kindlin-2 in HeLa cells. FHL1 (green) was mainly colocalized with kindlin-2 (red) in focal adhesion sites. Bars, 10 µm. **(F)** Indicated truncates of kindlin-2 were constructed according to the functional domains. **(G)** HeLa cells were transfected with the indicated truncates of GFP–kindlin-2. Cell lysates were then incubated with GST or GST-FHL1 in vitro for GST pulldown assays followed by immunoblotting using an anti-GFP antibody. **(H)** GST pulldown assays were performed using HeLa cells lysates transfected with Flag–kindlin-2 expression vector. GST-FHL1 fragments were purified using Glutathione Sepharose 4B beads, and then beads were incubated with HeLa cell lysate at 4°C overnight. Kindlin-2 was analyzed by Western blotting using an anti-Flag antibody.

Importantly, FHL1 nuclear translocation induced by Src could be observed by the use of the anti–p-Tyr149–FHL1 and anti–p-Tyr272–FHL1 antibodies for immunofluorescence (Fig. 5 G), suggesting that the nuclear translocated FHL1 is phosphorylated. Moreover, we detected FHL1 phosphorylation at different time points using the p-FHL1 antibody to track the process of p-FHL1 translocation. As shown in Fig. S3, p-FHL1 appeared at focal adhesions in the cells at 12 h after overexpressing Src-WT and Src-CA, and p-FHL1 gradually translocated to the nucleus. Indeed, most p-FHL1 was localized in the nucleus at 48 h after overexpressing Src-WT and Src-CA. Moreover, we found that Src was highly activated in H1299 cells (Fig. 2 G), and correspondingly, FHL1 was abundant in the nuclei of H1299 cells as visualized by immunofluorescent staining (Fig. 5 H). However, treatment of cells with PP2 led to decreased nuclear translocation of endogenous FHL1 (Fig. 5 H). In addition, cell fractionation analysis showed that the expression level of endogenous FHL1 was high in the nuclei of H1299 cells and that treatment with PP2 resulted in a significant reduction of FHL1 in the nuclei (Fig. 5 I). Collectively, these data demonstrate that Src phosphorylation caused the nuclear translocation of FHL1.

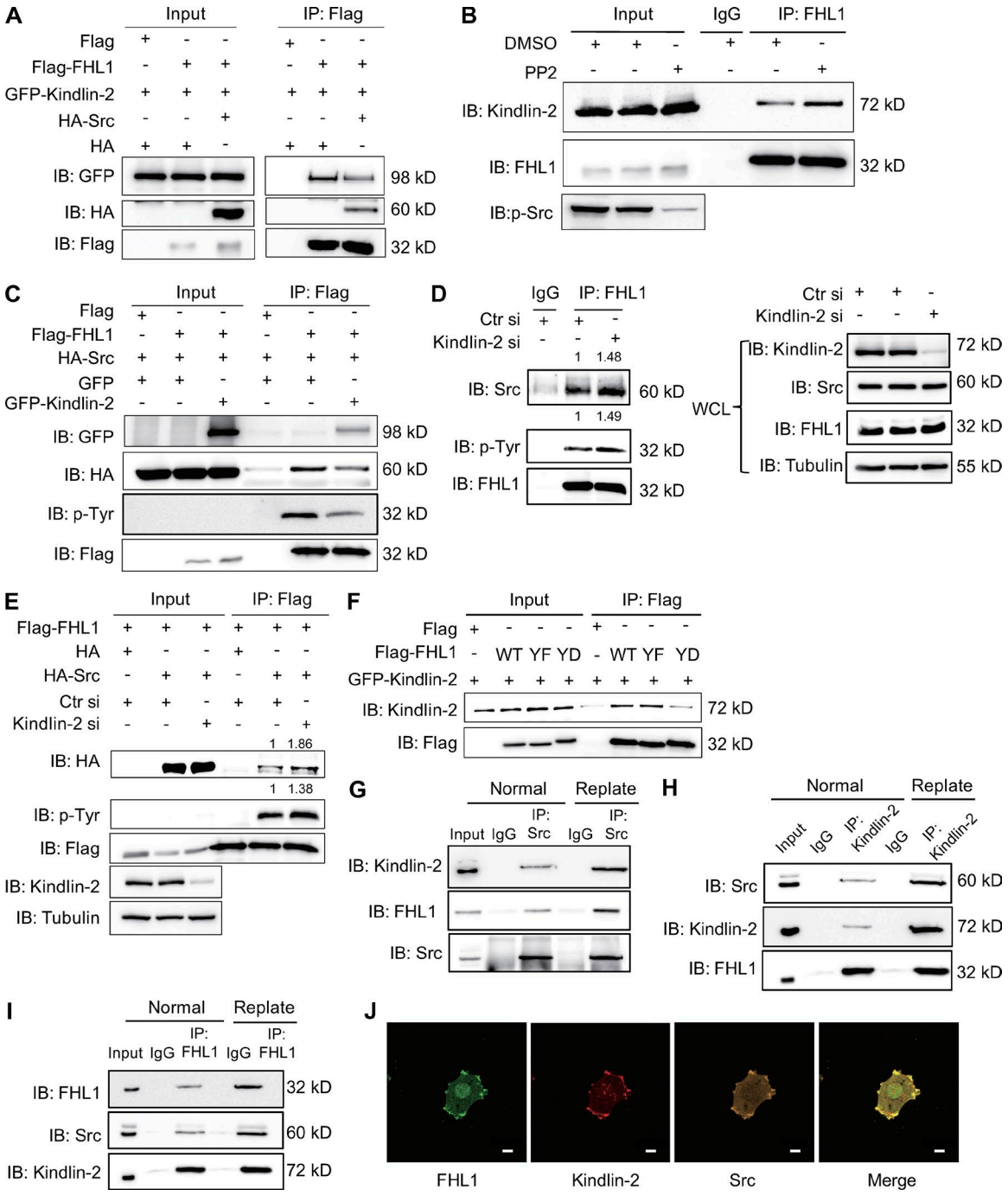

Figure 4. **Kindlin-2 competes with Src to interact with FHL1. (A)** HeLa cells were transfected with indicated plasmids. Cell lysates were immunoprecipitated with anti-Flag M2 beads followed by immunoblotting (IB) with indicated antibodies. **(B)** H1299 cells were pretreated with DMSO or PP2 for 12 h, and the interaction between kindlin-2 and FHL1 was analyzed. **(C)** HeLa cells were transfected with indicated plasmids. Cell lysates were immunoprecipitated with anti-Flag M2 beads followed by immunoblotting with indicated antibodies. **(D)** H1299 cells were transfected with control siRNA or kindlin-2 siRNA for 48 h, the interaction between Src and FHL1 was analyzed, and p-Tyr of FHL1 was determined. WCL, whole-cell lysate. **(E)** HeLa cells were transfected with indicated plasmids and siRNAs. Cell lysates were immunoprecipitated with anti-Flag M2 beads followed by immunoblotting with indicated antibodies. **(F)** HeLa cells were transfected with FHL1-WT, FHL1-Y149-272F (YF; phosphorylation-deficient mutant), or FHL1-Y149-272D (YD; phosphomimetic mutant) expression vectors together with GFP–kindlin-2. Cell lysates were immunoprecipitated with anti-Flag M2 beads that were immunoblotted with kindlin-2 antibody. **(G–I)** H1299 cells were starved and kept in suspension for 30 min or replated on FN-coated dishes for 1 h. Then, cells were lysed and immunoprecipitated with kindlin-2, Src, or FHL1 antibodies followed by immunoblotting with indicated antibodies. **(J)** Visualization of endogenous FHL1, kindlin-2, and endogenous Src in H1299 cells. FHL1 (green) was mainly colocalized with kindlin-2 (red) and Src (orange) in focal adhesion sites. Bars, 10 µm.

FHL1 phosphorylation by Src promotes lung cancer cell growth

It is well known that Src functions as an oncogene, whereas FHL1 is considered a tumor suppressor (Asada et al., 2013). Given that Src phosphorylates FHL1 and promotes FHL1 nuclear translocation, phosphorylation of FHL1 may change its tumor-suppressive role. To test the hypothesis, an FHL1 phosphorylation site double mutant was generated. Subsequently, the effects

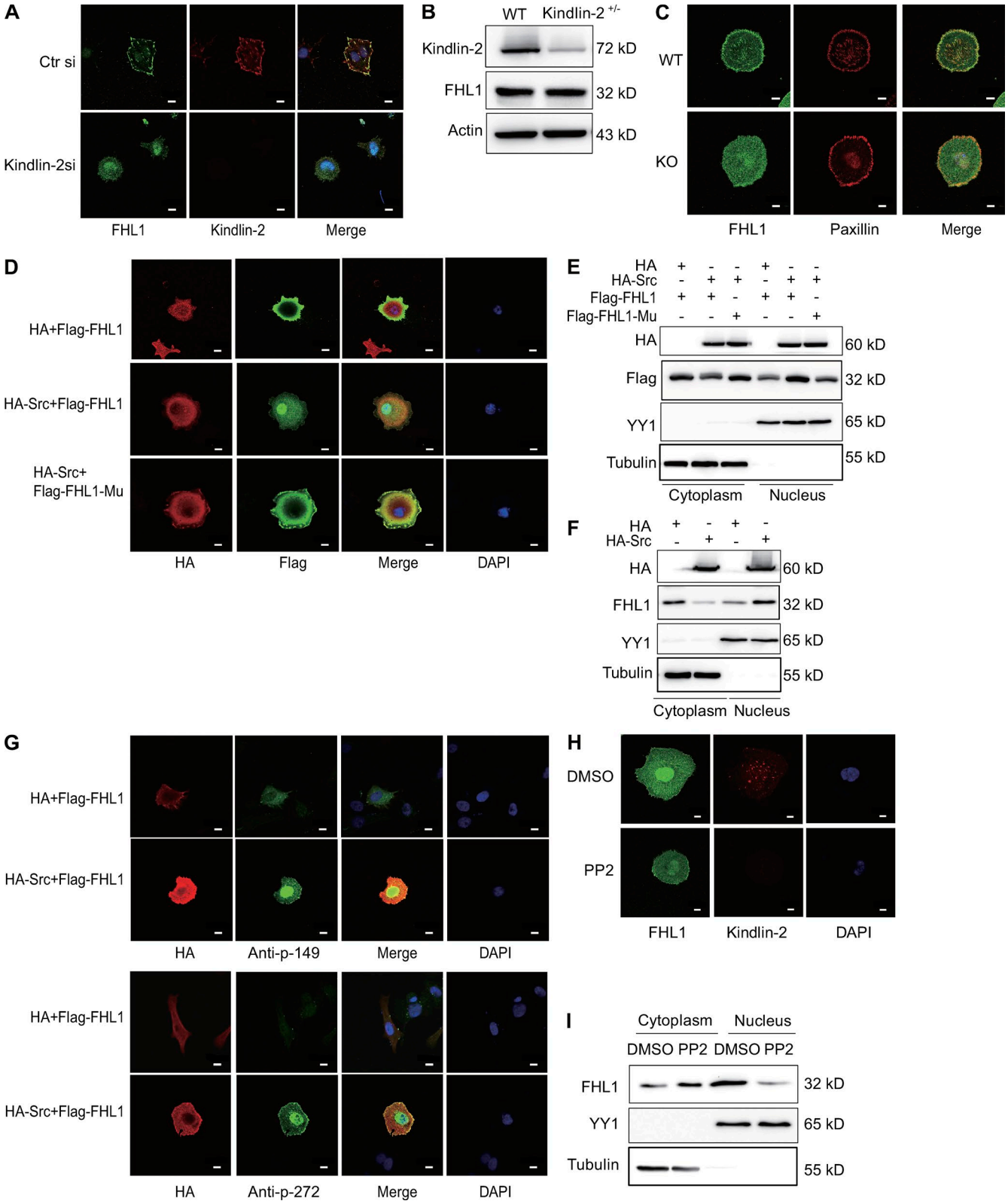

Figure 5. **Kindlin-2 and c-Src regulate the subcellular localization of FHL1. (A)** HeLa cells transfected with the control siRNA or kindlin-2 siRNA were replated on FN-coated coverslips for 4 h and stained with anti–kindlin-2 and anti-FHL1 antibodies. The nuclei were stained with DAPI. **(B)** Kindlin-2 depletion of *kindlin-2*$^{+/-}$ MEF cells was confirmed by Western blotting. (C) WT and *kindlin-2*$^{+/-}$ MEF cells were replated on FN-coated coverslips for 4 h and immunoreacted with anti–kindlin-2, anti-FHL1, and antipaxillin. Localization of kindlin-2, FHL1, and paxillin were observed by confocal microscopy under a 63× objective. KO, knockout. **(D)** Indicated plasmids were transfected into HeLa cells for 48 h, and then cells were immunoreacted with anti-HA and anti-Flag antibodies. The nuclei were stained with DAPI. Expression and localization of HA-Src and Flag-FHL1 were observed under a confocal microscope with a 63× objective. **(E and F)** HeLa cells were transfected with indicated plasmids for 48 h. Then, cells were fractionated and blotted with the indicated antibodies. Tubulin and YY1 were examined to indicate the cytoplasmic and nuclear extracts, respectively. **(G)** Indicated plasmids were transfected into HeLa cells

of FHL1-Y149-272 phosphorylation on lung cancer cell proliferation and tumor growth in mice were investigated. We first established H1299 cells that stably expressed Flag-tagged FHL1-WT, FHL1-Y149-272F (phosphorylation-deficient mutant) or FHL1-Y149-272D (phosphomimetic mutant; Fig. 6 A). Consistent with a previous study, overexpressed FHL1-WT caused a significant decrease in H1299 cell growth as examined by the WST1 assay, whereas cells expressing the phosphomimic mutant FHL1-Y149-272D markedly promoted lung cancer cell growth as compared with the FHL1-WT (Fig. 6 B; Niu et al., 2012). In contrast, expression of FHL1-Y149-272F significantly decreased H1299 cell proliferation. From day 4, the statistical difference was found between any two groups (Fig. 6 B). Next, the effects of FHL1 phosphorylation on anchorage-dependent and anchorage-independent growth were tested. The results from the colony formation assay and soft agar colony formation assay showed that FHL1-WT inhibited colony formation for H1299 cells as compared with the control group. Moreover, overexpression of FHL1-Y149-272D promoted lung cancer cell colony formation as compared with the FHL1-WT, whereas stably overexpressed FHL1-Y149-272F decreased H1299 cell colony formation (Fig. 6, C and D). Furthermore, we demonstrated that mutant FHL1-Y149-272D promoted lung cancer cell migration as compared with FHL1-WT. In contrast, overexpression of FHL1-Y149-272F inhibited H1299 cell migration (Fig. S4, A and B). To investigate the role of FHL1 phosphorylation in tumor growth, H1299 cells stably overexpressing FHL1-WT, FHL1-Y149-272F, or FHL1-Y149-272D were generated separately, and cells were injected subcutaneously into nude mice. As shown in Fig. 6 (E–G), cells expressing FHL1-Y149-272D displayed a faster tumor growth rate and larger tumor volumes than those of FHL1-WT. However, cells expressing FHL1-Y149-272F displayed a slower tumor growth rate and smaller tumor volumes than those of the FHL1-WT. To reveal the mechanism by which phosphorylation of FHL1 modulated lung cancer cell growth, cell cycle analysis was performed. Consistent with a previous study (Niu et al., 2012), overexpression of FHL1-WT induced G1/S cell cycle arrest, and cells expressing FHL1-Y149-272F resulted in a larger reduction in the proportion of cells in the G1 phase. Moreover, overexpression of FHL1-Y149-272D increased the proportion of cells in S phase as compared with the FHL1-WT (Fig. 6, H and I). The statistical difference of cells proportion in G1 and S phase was found between any two groups (Fig. 6 I). A recent study suggests that FHL1 might induce apoptosis (Cao et al., 2016), and to test this possibility, H1299 stable cell lines expressing FHL1-WT, FHL1-Y149-272F, and FHL1-Y149-272D were stained with propidium iodide (PI) and annexin V–phycoerythrin and then assessed by flow cytometry. As shown in Fig. 6 (J and K), FHL1 or its mutants showed no impact on H1299 cell apoptosis. Altogether, these data indicate that FHL1 phosphorylation promotes lung cancer cell growth both in vitro and in vivo.

Phosphorylated FHL1-promoted tumor growth is mediated by the transcription factor BCLAF1

Given that Src promotes FHL1 nuclear translocation and drives FHL1 from a tumor suppressor to a tumor promoter, we thus wanted to understand the molecular mechanism underlying the effect of phosphorylated FHL1 in promoting lung cancer cell growth. To this end, we attempted to identify the associated nuclear proteins that mediate the effect of phosphorylated FHL1. Nuclear extracts of H1299 cells overexpressing Flag-FHL1 and HA-Src were prepared, and a co-IP assay was performed with anti-Flag M2 beads. Proteins coimmunoprecipitated together with nuclear FHL1 were analyzed by mass spectrometry. Among the associated proteins identified, transcription factor BCLAF1 displayed a high score in protein association and was selected for further characterization (Table S1). To clarify whether nuclear FHL1 interacts with BCLAF1, we performed a series of protein interaction assays. Flag-BCLAF1 and HA-Src were cotransfected into HeLa cells, and then co-IP assays were performed using anti-Flag M2 beads or an anti-HA antibody followed by immunoblotting using FHL1 or Flag antibodies, respectively. These results show that exogenous FHL1 physically interacted with exogenous BCLAF1 (Fig. 7, A and B). Moreover, endogenous BCLAF1 and FHL1 also showed a strong association (Fig. 7, C and D). To examine whether phosphorylation of FHL1 is required for this interaction, FHL1-WT, FHL1-Y149-272F, or FHL1-Y149-272D were transfected into H1299 cells, and then a co-IP was performed. As shown in Fig. 7 E, the phosphomimic mutant FHL1-Y149-272D showed a stronger interaction with endogenous BCLAF1 as compared with that of the FHL1-WT. In contrast, FHL1-Y149-272F showed no ability to interact with BCLAF1. These data imply that only phosphorylated FHL1 interacts with BCLAF1. In support, immunofluorescent staining showed that overexpression of Src induced FHL1 translocation into the nuclei, and once there, FHL1 was colocalized with endogenous BCLAF1 (Fig. 7 F). Collectively, these data strongly indicate that phosphorylated FHL1 translocates into the nuclei and interacts with BCLAF1.

Interestingly, BCLAF1 is known to play important roles in diverse biological processes including apoptosis (Kasof et al., 1999; Lamy et al., 2013), posttranscriptional processes (Sarras et al., 2010), lung development (McPherson et al., 2009), and T cell activation (Kong et al., 2011). Recently, a BCLAF1 isoform was found to promote the growth of colon cancer cells (Zhou et al., 2014). As reported by Zhou et al. (2014), a larger band of 140 kD (L isoform) and a smaller one of 110 kD (T isoform) were readily detected in colon cancer cells, and the BCLAF-L isoform promotes tumorigenesis of human colon cancer cells. Interestingly, H1299 cells were also found to mainly express the L isoform of BCLAF1, which led us to examine whether BCLAF1 contributed to the tumor-promoting effect of phosphorylated FHL1. To this end, the L isoform of BCLAF1 was knocked down by three different siRNAs, and results showed that these three siRNAs against BCFAL1 worked equally (Fig. 7 G). Then, the possible involvement of BCFAL1 in phosphorylated FHL1-promoted tumor growth was investigated. The results showed that knockdown of BCLAF1 inhibited FHL1-Y149-272D–induced cell growth and colony formation as determined by WST-1 (Figs. 7 H and S4 C) and colony

for 48 h, and then cells were immunoreacted with anti-HA or anti–p-Tyr149–FHL1 or anti–p-Tyr272–FHL1 antibodies. The nuclei were stained with DAPI. **(H)** H1299 cells were pretreated with DMSO or PP2 for 12 h followed by staining with anti-FHL1 and anti–kindlin-2 antibodies. Then, the expression and localization of FHL1 and kindlin-2 were determined by confocal microscopy under a 63× objective. Bars, 10 µm. **(I)** H1299 cells were pretreated with DMSO or PP2 for 12 h followed by immunoblotting with indicated antibodies.

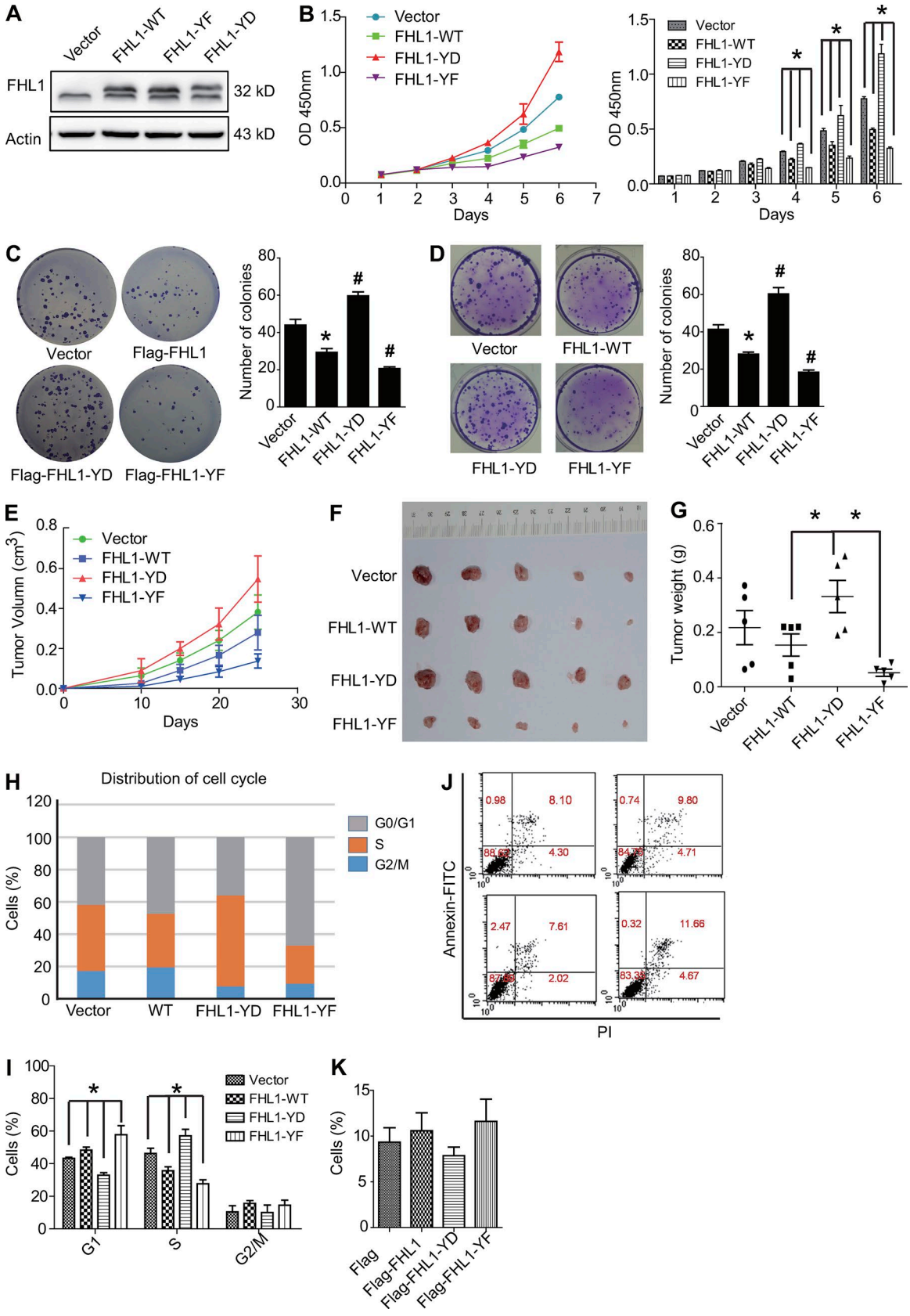

Figure 6. **FHL1 phosphorylation promotes lung cancer cell growth. (A)** H1299 cells stably expressing FHL1-WT, FHL1-Y149-272D (FHL1-YD), and FHL1-Y149-272F (FHL1-YF) were established, and the expression of target proteins was verified by Western blot analysis using FHL1 antibody. **(B)** WST1 assay was performed to examine the effect of FHL1 phosphorylation on H1299 cell growth. The cells were seeded into 96-well plates, and the absorbance at 450 nm was measured at the indicated time points. **(C)** The effect of FHL1 phosphorylation on the anchorage-dependent growth of H1299 cells was analyzed. Colonies are shown in the photographs. **(D)** The effect of FHL1 phosphorylation on the anchorage-independent growth of H1299 cells was analyzed.

formation assays (Fig. 7 I). These data clearly indicate that tumor growth promoted by phosphorylated FHL1 requires BCLAF1. Furthermore, FHL1-Y149-272D regulation of cell cycle G1/S transition also required BCLAF1 (Figs. 7 J and S4 D). In these experiments, the results from one siRNA were presented; however, the other two siRNAs were also used for experiments, and almost identical results were obtained (not depicted). To further determine the role of BCLAF1 in phosphorylated FHL1-induced tumor growth, H1299 cells stably overexpressing FHL1-Y149-272D with depleted BCL AF1 by siRNA were injected subcutaneously into nude mice, and tumor growth was observed. As shown in Fig. 7 (K–M), cells expressing FHL1-Y149-272D displayed larger tumor volumes and were heavier than those of the FHL1-WT and vector groups. However, cells depleted in BCLAF1 displayed smaller tumor volumes and were lighter than those with the FHL1-Y149-272D mutations. Collectively, these results suggest that BCLAF1 is required for mediating the effect of phosphorylated FHL1 to promote tumor growth.

Enhanced FHL1 phosphorylation was observed in lung adenocarcinomas

Given that phosphorylated FHL1 regulates lung cancer progression in cells and mouse xenografts as shown in Fig. 6, we next examined whether the phosphorylation of FHL1 can be detectable in the lung adenocarcinoma patients and whether the level of phosphorylated FHL1 is higher in lung adenocarcinomas as compared with the normal lung tissues. To this end, we examined the phosphorylated and total FHL1 levels by immunohistochemical staining in both normal and tumor tissues from the same patient using consecutive tissue sections of the lung adenocarcinoma. The results from three patients of a pilot study showed that phosphorylated FHL1 was present, localized in the nuclei, and remarkably increased in tumor tissue as compared with normal tissues (Fig. 8, A–C). In contrast, total FHL1 expression was evidently decreased in tumor tissues, which is consistent with a previous study (Fig. 8, A–C; Niu et al., 2012). We then performed analyses of different databases, including Kaplan–Meier Plotter analysis database (Lanczky et al., 2016) and TCGA database (Anaya, 2016), and found that higher FHL1 expression correlated with a better overall survival in lung cancer and that this relationship is more obvious in lung adenocarcinoma (Fig. S5 A). However, correlation between FHL1 phosphorylation and patient survival in lung cancer needs further investigation. To further confirm the role of phosphorylated FHL1 in cancer, we used the tissue chip of multiple organ cancer to detect p-FHL1 and total FHL1 expression. The results showed that in addition to lung cancer, p-FHL1 is also remarkably increased in liver, gastric, rectal, and esophagus cancer, accompanied by the down-regulation of total FHL1 expression (Fig. S5 B). These results demonstrate that total FHL1 level in tumors decreased and that a fraction of the phosphorylated FHL1 translocates into the nuclei and is tumorigenic.

Discussion

FHL1, a tumor suppressor characterized by its ability to inhibit tumor cell growth, has been reported to associate with focal adhesions and the actin cytoskeleton (Brown et al., 1999). Moreover, FHL1 can shuttle between the nucleus and cytoplasm in an integrin-dependent manner (Robinson et al., 2003). Despite these findings, little is known about the underlining mechanism regarding the role of FHL1 in tumor progression or the physiological processes responsible for the regulation of FHL1 localization and translocation in cells (Zheng and Zhao, 2007). This study demonstrates that Src interacts with FHL1 and mediates its phosphorylation, and this causes FHL1 to translocate into the nucleus and interact with BCLAF1. Importantly, phosphorylated FHL1 abolishes the tumor-suppressive role of FHL1 and actually promotes tumor growth. However, when the focal adhesion molecule kindlin-2 is raised in cells, FHL1 is recruited to focal adhesions by interacting with kindlin-2. As a result, both the interaction between FHL1 and Src and the phosphorylation of FHL1 are suppressed, and the tumor suppressor function of FHL1 is maintained. Collectively, FHL1 plays a dual role in the regulation of tumor cell growth, a role that is dependent on the level of kindlin-2 and Src in cells (Fig. 8 D).

FHL1 is down-regulated in a variety of cancers, and diminished FHL1 expression likely contributes to increased metastasis and decreased survival in cancer patients. In addition, it was reported that FHL1 inhibits tumor cell growth by transcriptional regulation of TGF-β–responsive genes and by corepressing ER transcriptional activity (Ding et al., 2009, 2011; Lin et al., 2009). Recently, our study showed that FHL1 causes radioresistance in cancer cells by inhibiting CDC25C activity (Xu et al., 2017), supporting the notion that FHL1 may be a double-edged sword in tumor progression.

To date, little is known about the posttranslational modification of FHL1 and how modified FHL1 may play a role in cancer progression. In this study, we demonstrated that FHL1 could be phosphorylated by Src and subsequently translocated into the nucleus. We found that Src phosphorylates FHL1 at Y149 and Y272, demonstrating that FHL1 is a bona fide novel substrate of Src. However, we speculate that other sites may be phosphorylated in response to different kinase events or even in different cell types. Notably, phosphorylated FHL1 did not inhibit but instead promoted tumor cell growth in vitro and in vivo as compared with WT FHL1. In support, the level of phosphorylation of FHL1 increased in human lung adenocarcinomas, although total FHL1 expression was down-regulated in tumor tissue as compared with normal tissue. To our knowledge, this is the first study to identify that posttranslational modification of FHL1 could change the function of FHL1 from a tumor cell growth suppressor to a tumor cell growth promoter, which expands and deepens our current understanding of FHL1 function during cancer progression.

The tyrosine kinase Src is known to play a critical role in various human cancers (Ishizawar and Parsons, 2004). However,

Representative images of colonies grown in soft agar. Values shown are means ± SD of triplicate measurements. *, $P < 0.05$ versus vector group; #, $P < 0.05$ versus FHL1-WT. **(E–G)** Phosphorylated FHL1 promotes tumor growth in nude mice. Mice were injected with stable H1299 and control cells. Tumor growths in xenografted nude mice were measured and plotted (E). The xenograft tumors were dissected and photographed at day 25 (F). Mean tumor weights were measured at day 25. Statistical analyses were performed by Student's *t* tests. $n = 5$ (G). **(H and I)** Effect of FHL1 phosphorylation on the distribution of cell cycle was observed in H1299 cells through cell cycle analysis (H). **(J and K)** Apoptosis potential of FHL1 phosphorylation in H1299 cells was examined by PI and annexin V–FITC double staining through flow cytometry. Statistical analyses were performed by one-way ANOVA. Values shown are means ± SD of triplicate measurements (K). *, $P < 0.05$.

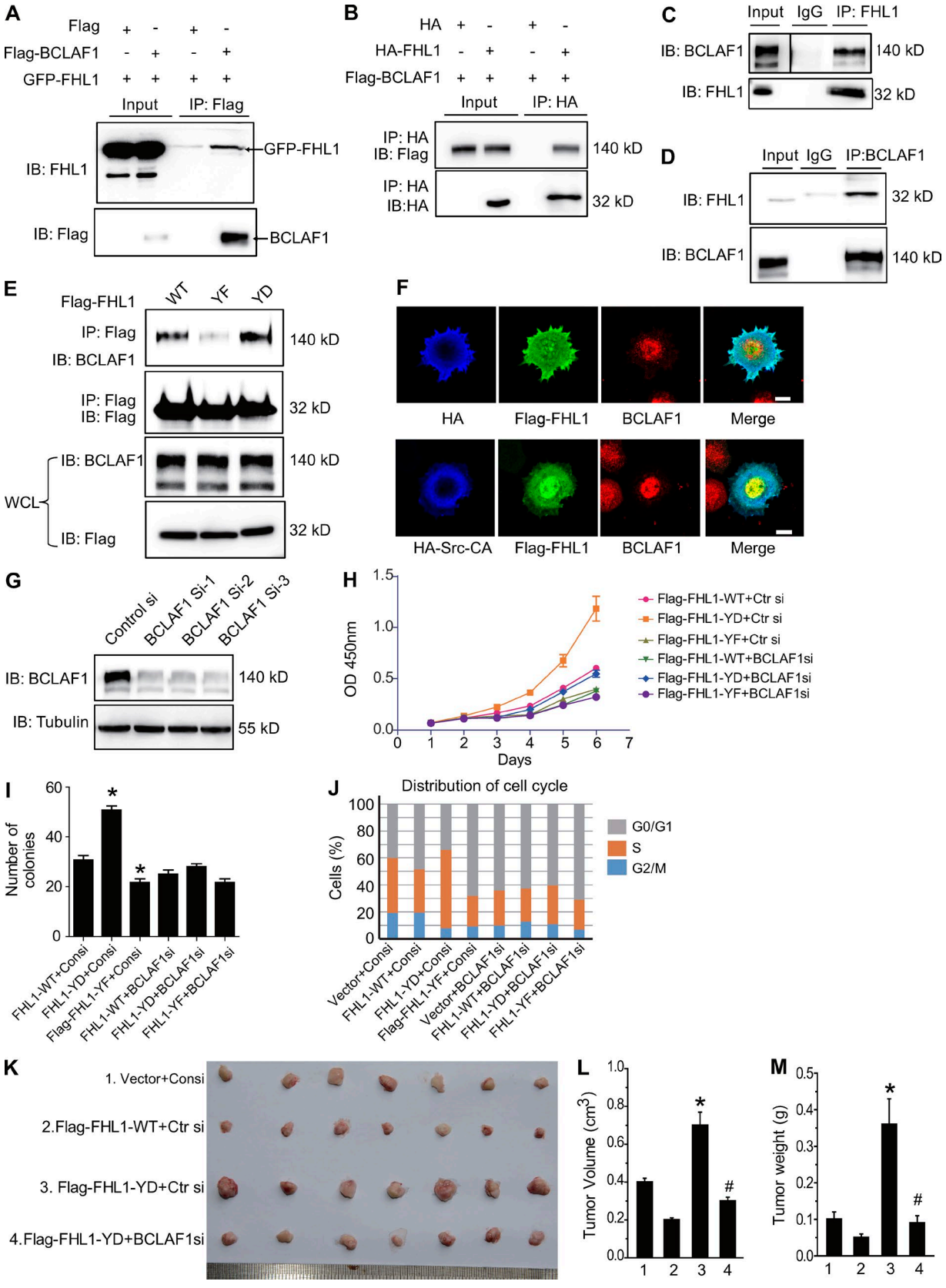

Figure 7. **The tumor growth effect of phosphorylated FHL1 is dependent on BCLAF1. (A and B)** The exogenous interaction between FHL1 and BCLAF1 was analyzed by co-IP. HeLa cells were transfected with indicated plasmids. Cell lysates were immunoprecipitated with anti-Flag M2 beads followed by immunoblotting using FHL1 antibody (A). HeLa cells transfected with indicated plasmids were lysed and immunoprecipitated with anti-HA antibody followed by immunoblotting (IB) using Flag antibody (B). **(C and D)** The endogenous interaction between FHL1 and BCLAF1 was analyzed by co-IP. Co-IP assays were performed using lysates from H1299 cells with control IgG or anti-FHL1 antibody followed by immunoblotting with anti-BCLAF1 (C). H1299 cells

the molecular mechanism underlying Src involvement in tumor progression remains elusive. This study identified a novel mechanism accounting for Src as an oncogene that alters the tumor-suppressive role of FHL1 through phosphorylation. Interestingly, a previous study showed that v-Src transformation in cells blocks FHL1 expression and that suppression of FHL1 is required for Src to promote tumor cell growth (Shen et al., 2006). Although we did not show that Src affects the expression of FHL1, Src phosphorylates and induces the nuclear translocation of FHL1, which may also be essential for Src to perform a tumor-promoting function. Collectively, FHL1 may play an important role in Src-mediated tumor progression.

In this study, FHL1 was found to be colocalized with Src mainly at focal adhesions in cells. It is known that FHL1 localizes to focal adhesions and interacts with focal adhesion proteins including paxillin and talin (Kwapiszewska et al., 2008; Veith et al., 2012). In addition, it has been reported that FHL1 regulates integrin-mediated myoblast adhesion, spreading, and migration (Robinson et al., 2003). However, how FHL1 is recruited to focal adhesions remains unknown. Kindlin-2, an integrin-interacting protein, has been reported to recruit migfilin, a LIM domain–containing protein to focal adhesions. By siRNA knockdown and using kindlin-2$^{+/-}$ MEF cells, we identified that kindlin-2 is also indispensable for FHL1 localization to focal adhesions. Interestingly, Src, FHL1, and kindlin-2 form a tertiary complex at focal adhesions. Our previous study demonstrated that kindlin-2 phosphorylation by Src enhances Src activity (Liu et al., 2015). It is tempting to hypothesize that kindlin-2 recruits FHL1 to focal adhesions and constitutes a platform where Src becomes activated and phosphorylates FHL1, which subsequently translocates into the nucleus. However, when Src activity is low or the kindlin-2 level is high in cells, the interaction between FHL1 and Src is inhibited. This results in suppressed phosphorylation and nuclear translocation of FHL1, leading to stable localization of FHL1 at focal adhesions. This suggests that the physiological and pathological functions of FHL1 may be dependent on its phosphorylation state.

Previous studies indicated that FHL1 could be localized to focal adhesions and shuttle between the nucleus and cytoplasm (Brown et al., 1999; Lin et al., 2009). Other investigations showed that the translocation of FHL1 to the nucleus affects transcription of some genes (Ding et al., 2011). This study demonstrates that Src induces FHL1 nuclear translocation. We further identified BCLAF1 as a previously unrecognized FHL1-interacting protein in the nucleus. BCLAF1 is a nuclear protein that was previously identified to interact with adenoviral bcl-2 homologue E1B19K (Kasof et al., 1999) and induces apoptosis and suppresses gene transcription. However, the role of BCLAF1 in the apoptotic pathway remains controversial. Knockout of BCLAF1 did not show any obvious defects in apoptosis (McPherson et al., 2009). Recently, an interesting study demonstrated that BCLAF1 promotes colon cancer cell growth but does not affect cell death (Zhou et al., 2014). This study found that knockdown of BCLAF1 inhibits phosphorylated FHL1-induced tumor cell growth and colony formation, indicating that BCLAF1 mediates phosphorylated FHL1-induced tumor progression. However, further investigations need to be performed to uncover the underlying mechanisms of how phosphorylated FHL1 cooperated with BCLAF1 to promote lung cancer cell proliferation.

In summary, we identified that FHL1 is a novel substrate of Src. FHL1 becomes an oncogenic protein through Src-mediated posttranslational modification. Src interacts with and phosphorylates FHL1, which subsequently leads to FHL1 nuclear translocation in which FHL1 interacts with the transcription factor BCLAF1. Phosphorylated FHL1 cooperates with BCLAF1 and functions as a tumor cell growth promoter.

Materials and methods

Plasmids and siRNAs

The Flag-tagged FHL1 expression plasmid was cloned into a pcDNA3 vector linked with Flag at the amino terminus. Plasmids encoding HA–Src-WT, HA–Src-KD (K298A), and HA–Src-CA (Y530F) were provided by B.-C. Oh (Chungbuk National University, Cheongju, South Korea; Shen et al., 2006). Full-length BCLAF1 was a gift from J. Tang (China Agricultural University, Beijing, China, Shao et al., 2016), which was subcloned into the pRK5 vector with an N-terminal Flag tag. Expression vectors encoding Flag–kindlin-2, HA–kindlin-2, and GFP–kindlin-2 were generated by inserting PCR-amplified kindlin-2 fragments into corresponding vectors (pCMV10-3×Flag, pCMV6-AC-3HA, and pEGFP-C3). Plasmids encoding GST- and His-fusion proteins were prepared by cloning PCR-amplified sequences into pGEX–4T-1 and pET28a (Novagen), respectively. Plasmid encoding His–kindlin-2 was constructed by cloning PCR-amplified sequences into pFastBac HT A (Invitrogen). Point mutations of FHL1 were generated using a Muta-direct mutagenesis kit (SBS Genetech Co., Ltd). All constructs were confirmed by DNA sequencing. The cDNA target sequence of siRNA for kindlin-2 (QIAGEN) was 5′-AAGCUGGUG GAGAAACUCG-3′. Three siRNAs targeting human BCLAF1 were designed and synthesized by RiboBio Co. And the sense-targeting sequences were as follows: sequence 1, 5′-GAUGAAGAGUCUAGA GUAUTT-3′; sequence 2, 5′-CGCAGAUCAGGGUAAAAGUTT-3′; and sequence 3, 5′-CCTTATGGGTACAGAGGAATT-3′. An irrelevant double-stranded RNA with the sense sequence 5′-UUCUCCGAACGU GUCACGU-3′ was used as control.

Antibodies and reagents

FHL1 (rabbit) antibody was purchased from ProteinTech. BCLAF1 (rabbit) and kindlin-2 (mouse) antibodies were from EMD Millipore. Kindlin-2 (rabbit), Flag (mouse), GFP (mouse), and HA (mouse)

were lysed, and equal amounts of protein lysates were immunoprecipitated with anti-BCLAF1 antibody or IgG and probed with anti-FHL1 antibody (D). **(E)** H1299 cells were transfected with FHL1-WT or FHL1-Y149-272F (FHL1-YF) mutant or FHL1-Y149-272D (FHL1-YD) mutant expression vectors. Cell lysates were immunoprecipitated with anti-Flag M2 beads that were immunoblotted with BCLAF1 antibody. WCL, whole-cell lysate. **(F)** Visualization of Flag-FHL1, HA-Src, and endogenous BCLAF1 in HeLa cells. FHL1 (green) was colocalized with BCLAF1 (red) mainly in the nucleus. Bars, 10 µm. **(G)** The efficiency of BCLAF1 siRNAs on endogenous BCLAF1 protein in H1299 cells. **(H)** A WST1 assay was performed when BCLAF1 was knocked down in H1299 cells stably expressing FHL1-WT, FHL1-Y149-272D, and FHL1-Y149-272F mutant. **(I)** The effect of BCLAF1 depletion by siRNA on the colony formation potential of H1299 cells. *, $P < 0.05$ versus FHL1-WT + control small interfering group. **(J)** The effect of BCLAF1 depletion by siRNA on the distribution of cell cycle of H1299 cells was analyzed by flow cytometry. **(K–M)** Mice were injected with stable H1299 cells, and control cells were transfected with BCLAF1 siRNA or control siRNA. Xenograft tumors were dissected and photographed at day 20 (K). The tumor mass (L) and mean tumor weights were measured (M). Values shown are means ± SD. $n = 7$. *, $P < 0.05$ versus vector group; #, $P < 0.05$ versus FHL1-Y149-272D.

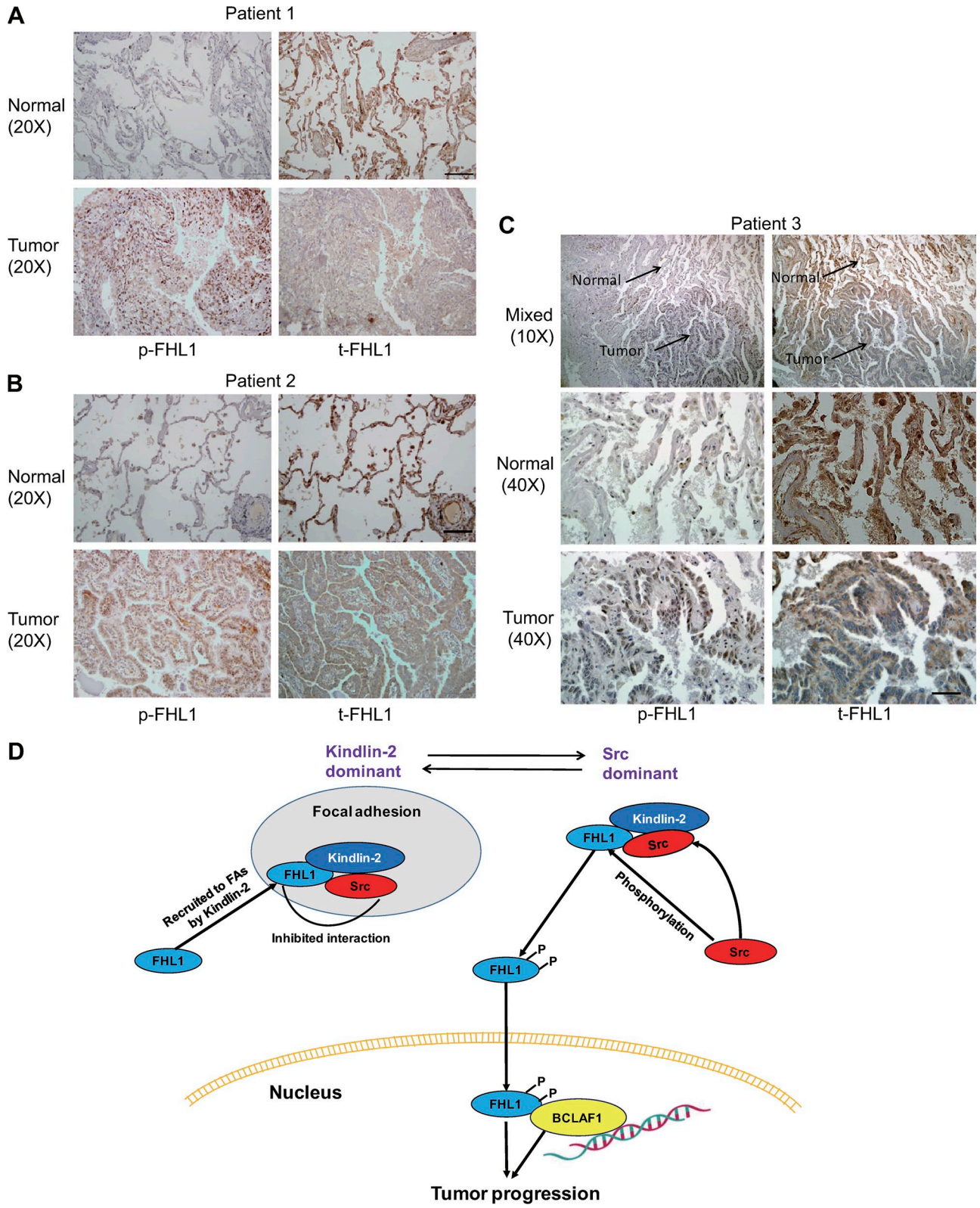

Figure 8. **Phosphorylation of FHL1 was increased in human tissues with lung adenocarcinoma. (A and B)** Phosphorylation of FHL1 and total FHL1 expression both in normal and lung adenocarcinoma tissue from two patients was determined by immunohistochemistry using consecutive sections from the same tissue. Bars, 100 µm. **(C)** Phosphorylation of FHL1 and total FHL1 expression in the lung tissues from a third patient with lung adenocarcinoma was determined by immunohistochemistry using consecutive sections. The normal and tumor tissues were resected and displayed on one section. Bars: (10× objective) 200 µm; (40× objective) 50 µm. **(D)** A hypothetical model for regulation of FHL1 phosphorylation and localization. Src interacts with FHL1 and induces the phosphorylation of FHL1. Upon phosphorylation, FHL1 immediately translocates into the nucleus, where FHL1 promotes tumor cell growth by interacting and cooperating with transcription factor BCLAF1. When kindlin-2 is dominant in cells or is overexpressed, FHL1 is recruited to focal adhesions (FAs) and forms a complex with kindlin-2 and Src. However, the interaction of Src and FHL1 is suppressed in this state.

antibodies as well as anti-flag M2 beads were purchased from Sigma-Aldrich. Src (mouse), β-actin (mouse), YY1 (mouse), and β-tubulin (mouse) were obtained from Santa Cruz Biotechnology, Inc. Anti–p-Src Y416 and –p-Tyr–100 specifically recognizing phosphorylated tyrosine were purchased from Cell Signaling Technology. Antibodies specifically recognizing Y149- and Y272-phosphorylated FHL1 were produced by immunizing rabbits with phosphorylated peptides FFPKGEDFY^{P}CVTC and CHQEQVY^{P}CPDCAKK, respectively (Kang Wei Shi Ji). Secondary antibodies conjugated with Alexa Fluor 488, 568, or 633 for immunofluorescence were purchased from Invitrogen. Src family kinase inhibitor PP2 was purchased from Sigma-Aldrich. λ-Phosphatase (P0753S) was obtained from New England Biolabs, Inc.

Cell culture and transfection

MEFs were isolated from E12.5 embryos and cultured in DMEM supplemented with 10% FBS, penicillin-streptomycin, and 2 mM L-glutamine using standard techniques. Human cervical carcinoma cells HeLa cells were cultured in DMEM supplemented with 10% FBS. H1299 cells were grown in RPMI 1640 (Invitrogen) supplemented with 10% FBS. Cells were transfected with RNAiMAX or Lipofectamine 2000 (Invitrogen) or PEI (Polyscience) following the manufacturer's protocol.

GST pulldown assay

GST-fusion proteins and His-FHL1 were expressed in *E. coli* BL21 (Tiangen Biotechnology), and GST-fusion proteins were purified with Glutathione Sepharose 4B beads (Pharmacia Medtech). Then, the cell lysates or His-FHL1 were incubated with Glutathione Sepharose 4B beads that were precoated with GST or GST-fusion proteins for 12 h at 4°C under rotation. His–kindlin-2 was expressed in Sf9 insect cells and purified by HisTrap histidine-tagged protein columns (GE Healthcare). Then, GST-fusion proteins were incubated with His-Select High Flow nickel affinity gel (Sigma-Aldrich) that was precoated with His–kindlin-2 for 12 h at 4°C under rotation. Then, beads were washed with RIPA buffer for extended times, and proteins were eluted, followed by Western blotting.

IP and immunoblotting

Cells were collected and lysed by RIPA buffer (50 mM Tris-HCl, 150 mM NaCl, pH 7.4, 0.5% sodium deoxycholate, 1% NP-40, 0.1% SDS, 1 mM Na_3VO_4, and 100 mM NaF) with protease inhibitor cocktail on ice. IPs were performed using indicated primary antibodies and protein A/G–agarose beads (Santa Cruz Biotechnology, Inc.) or anti-Flag M2 beads (Sigma-Aldrich) at 4°C. Then, immune complexes were washed for extended times with RIPA buffer and separated by SDS-PAGE gels. Transfer membranes were probed with indicated primary and secondary antibodies. The membranes were detected by the Super Signal chemiluminescence kit (Thermo Fisher Scientific).

In vitro kinase assay

GST-Src and His-FHL1 were produced and purified from BL21DE3 cells. His-FHL1 was incubated with GST or GST-Src that bound to Glutathione Sepharose 4B beads in kinase buffer containing 50 mM Tris-HCl, pH 7.8, 150 mM NaCl, 5 mM $MgCl_2$, 1.0 mM DTT, 5 mM ATP, and 0.25 mM Na_3VO_4 at 37°C for 1 h. Then, proteins were boiled and analyzed by Western blotting with indicated antibodies.

λ-Phosphatase treatment

λ-Phosphatase experiments were conducted as described previously (Pascreau et al., 2009). In brief, cells were lysed, and the extracts were incubated with 800 U λ-phosphatase in λ-phosphatase buffer with or without 2 mM $MnCl_2$ for 1 h at 30°C. The reaction was terminated with SDS sample buffer, and samples were resolved by SDS-PAGE, followed by Western blotting.

Immunofluorescence and confocal microscopy

The cells were cultured on coverslips and then washed with cold PBS twice, fixed in 4% paraformaldehyde, permeabilized with 0.1% NP-40, and stained with the indicated primary antibodies overnight at 4°C, followed by incubating with secondary antibodies conjugated with Alexa Fluor 488, 568, or 633 (Invitrogen). Cells were also stained with DAPI to visualize the nuclei. Intracellular localization was visualized using a confocal microscope (ZEISS).

Cellular viability assay

The effects of different FHL1 mutants on the viability of cells were assessed using the WST-1 assay as described previously (Große-Kreul et al., 2016). In brief, cells were seeded in 96-well plates in triplicates at the density of 1:1,000 cells/well. From the second day, cells were washed with serum-free medium and incubated with the WST-1 reagent (10 µl/well) in fresh serum-free medium at 37°C for 2 h. Then, the intensity of the color formation produced by viable cells was quantified by measuring the absorbance at 450 nm in a microplate reader (Biotec).

Anchorage-dependent and -independent cell proliferation assays

Anchorage-dependent cell proliferation was analyzed by crystal violet assay as described previously (Wang et al., 2008). In brief, 400 cells were seeded in six-well plates in triplicates with DMEM or RPMI 1640 medium supplemented with 10% FBS. After 10 or 14 d of growth, cells were fixed in 4% paraformaldehyde for 15 min and stained with 0.5% crystal violet for 15 min at room temperature. Pictures of the plates were taken using a digital camera (G9; Canon), and the number of colonies formed under each condition was counted and analyzed. For anchorage-independent growth assays, 5,000 cells were seeded in triplicate on 6-cm plates, with a bottom layer of 0.6% low–melting temperature agar in DMEM or RPMI 1640 and a top layer of 0.4% agar in DMEM or RPMI 1640. After 4 wk of growth, cells were stained with 1 mg/ml iodonitrotetrazolium chloride (Sigma-Aldrich) in PBS overnight at 37°C. Colonies that were >100 µm diameter were counted and analyzed.

Cell cycle analysis

Cell cycle analysis was determined by flow cytometry. In brief, cells were harvested and fixed in 70% ethanol overnight, washed in PBS, and incubated with RNaseA (0.2 mg/ml) in PBS for 1 h at 37°C. PI was added, and samples were analyzed on a FACSCalibur Flow Cytometer (BD). Data analysis was done using FlowJo software (BD).

Cell apoptosis assay

Cell apoptosis was determined by using the annexin V–FITC/PI cell apoptosis detection kit (BD) following the manufacturer's instructions. In brief, cells were trypsinized and washed with cold PBS and then resuspended in 1× binding buffer. Then, 5 µl of annexin V–FITC was added, and cells were incubated for 15 min at 37°C. PI was then added, and samples were analyzed on a FACSCalibur Flow Cytometer (BD).

Xenograft tumor formation in mice

H1299 cells (3×10^6) were counted and resuspended with 100 µl RPMI 1640 and injected subcutaneously into BALB/c female nude mice (purchased from the animal department of Peking University Health Science Center with approval of the Animal Care and Use Committee of Peking University Health Science Center), and then tumor sizes were measured at the indicated time. After certain days, tumors

were dissected when they reached ∼1 cm in diameter. Tumors were weighted and photographed.

Tissue samples and immunohistochemistry

Surgically removed lung adenocarcinoma tissues and adjacent normal tissues were collected from three patients at Peking University Third Hospital. The samples were used for immunohistochemical staining analysis. The experiments were approved by the Ethics Committee of Peking University Third Hospital. The tissue chips of multiple organ cancer were purchased from Shanghai Outdo Biotech Co. LTD.

Immunohistochemical staining for specific protein expression was performed on mouse tissue sections. In brief, sections (4 mm thick) were deparaffinized with xylene followed by rehydration in ethanol. Hydrogen peroxide (3%) was used to eliminate endogenous peroxidase. Sections were incubated overnight at 4°C with primary antibodies against FHL1 and p-FHL1. After extensive washing in PBS buffer, sections were then incubated for 30 min with secondary antibodies (Dako). The immunostaining was examined by a BX51 microscope (Olympus).

Statistical analysis

All experiments were performed in triplicate. Data are presented as means ± SD. Comparisons between two groups were made using two-tailed Student's *t* tests. Differences among more than two groups were compared using one-way ANOVAs. Pairwise comparisons were evaluated by the Student-Newman-Keuls procedure or Dunnett's T3 procedure when the assumption of equal variances did not hold. All statistical calculations were performed using SPSS software (13.0; IBM). P-values of <0.05 were considered statistically significant.

Online supplemental material

Fig. S1 shows mass spectrometry spectra analysis of the sites of c-Src–mediated FHL1 phosphorylation. Fig. S2 shows statistical analysis of Fig. 4 (D and E) as well as the subcellular localization of FHL1 regulated by kindlin-2. Fig. S3 shows time series of FHL1 phosphorylation induced by Src. Fig. S4 shows that phosphorylation of FHL1 promotes lung cancer cell migration and also shows statistical analysis of Fig. 7 (H and J). Fig. S5 shows analysis of FHL1 expression by database and tissue chip. Table S1 shows mass spectrometry spectra analysis of FHL1 interaction with BCAFL1 in the nucleus.

Acknowledgments

This study was supported by Ministry of Science and Technology of China grants 2016YFC1302103 and 2015CB553906, the National Natural Science Foundation of China grants 81230051, 30830048, 31170711, and 81321003, the Beijing Natural Science Foundation grants 7120002 and 7171005, the Ministry of Education 111 Project, Peking University grants BMU20120314 and BMU20130364, and a Beijing Education Bureau Leading Academic Discipline Project to H. Zhang. This work was also supported by a grant from the National Natural Science Foundation of China (81670626) to X. Wei.

The authors declare no competing financial interests.

Author contributions: X. Wei and X. Wang designed the research, did experimental work, analyzed data, and wrote the manuscript. Y. Yuan, Q. Sun, J. Zhan, J. Zhang, F. Li, Y. Tang, and L. Ding did experimental work. Q. Ye participated in study design. H. Zhang designed and conceptualized the research, supervised the experimental work, and wrote the manuscript.

Submitted: 9 August 2017
Revised: 19 December 2017
Accepted: 16 January 2018

References

Anaya, J. 2016. OncoLnc: linking TCGA survival data to mRNAs, miRNAs, and lncRNAs. *PeerJ Comput. Sci.* 2:e67. https://doi.org/10.7717/peerj-cs.67

Asada, K., T. Ando, T. Niwa, S. Nanjo, N. Watanabe, E. Okochi-Takada, T. Yoshida, K. Miyamoto, S. Enomoto, M. Ichinose, et al. 2013. FHL1 on chromosome X is a single-hit gastrointestinal tumor-suppressor gene and contributes to the formation of an epigenetic field defect. *Oncogene.* 32:2140–2149. https://doi.org/10.1038/onc.2012.228

Brown, S., M.J. McGrath, L.M. Ooms, R. Gurung, M.M. Maimone, and C.A. Mitchell. 1999. Characterization of two isoforms of the skeletal muscle LIM protein 1, SLIM1. Localization of SLIM1 at focal adhesions and the isoform slimmer in the nucleus of myoblasts and cytoplasm of myotubes suggests distinct roles in the cytoskeleton and in nuclear-cytoplasmic communication. *J. Biol. Chem.* 274:27083–27091. https://doi.org/10.1074/jbc.274.38.27083

Cao, W., J. Liu, R. Xia, L. Lin, X. Wang, M. Xiao, C. Zhang, J. Li, T. Ji, and W. Chen. 2016. X-linked FHL1 as a novel therapeutic target for head and neck squamous cell carcinoma. *Oncotarget.* 7:14537–14550.

Cowling, B.S., M.J. McGrath, M.A. Nguyen, D.L. Cottle, A.J. Kee, S. Brown, J. Schessl, Y. Zou, J. Joya, C.G. Bönnemann, et al. 2008. Identification of FHL1 as a regulator of skeletal muscle mass: implications for human myopathy. *J. Cell Biol.* 183:1033–1048. https://doi.org/10.1083/jcb.200804077

Cowling, B.S., D.L. Cottle, B.R. Wilding, C.E. D'Arcy, C.A. Mitchell, and M.J. McGrath. 2011. Four and a half LIM protein 1 gene mutations cause four distinct human myopathies: a comprehensive review of the clinical, histological and pathological features. *Neuromuscul. Disord.* 21:237–251. https://doi.org/10.1016/j.nmd.2011.01.001

Ding, L., Z. Wang, J. Yan, X. Yang, A. Liu, W. Qiu, J. Zhu, J. Han, H. Zhang, J. Lin, et al. 2009. Human four-and-a-half LIM family members suppress tumor cell growth through a TGF-beta-like signaling pathway. *J. Clin. Invest.* 119:349–361.

Ding, L., C. Niu, Y. Zheng, Z. Xiong, Y. Liu, J. Lin, H. Sun, K. Huang, W. Yang, X. Li, and Q. Ye. 2011. FHL1 interacts with oestrogen receptors and regulates breast cancer cell growth. *J. Cell. Mol. Med.* 15:72–85. https://doi.org/10.1111/j.1582-4934.2009.00938.x

Greene, W.K., E. Baker, T.H. Rabbitts, and U.R. Kees. 1999. Genomic structure, tissue expression and chromosomal location of the LIM-only gene, SLIM1. *Gene.* 232:203–207. https://doi.org/10.1016/S0378-1119(99)00125-0

Große-Kreul, J., M. Busch, C. Winter, S. Pikos, H. Stephan, and N. Dünker. 2016. Forced Trefoil Factor Family Peptide 3 (TFF3) Expression Reduces Growth, Viability, and Tumorigenicity of Human Retinoblastoma Cell Lines. *PLoS One.* 11:e0163025. https://doi.org/10.1371/journal.pone.0163025

Guarino, M. 2010. Src signaling in cancer invasion. *J. Cell. Physiol.* 223:14–26.

Guo, W., and F.G. Giancotti. 2004. Integrin signalling during tumour progression. *Nat. Rev. Mol. Cell Biol.* 5:816–826. https://doi.org/10.1038/nrm1490

Harburger, D.S., and D.A. Calderwood. 2009. Integrin signalling at a glance. *J. Cell Sci.* 122:159–163. https://doi.org/10.1242/jcs.018093

Ishizawar, R., and S.J. Parsons. 2004. c-Src and cooperating partners in human cancer. *Cancer Cell.* 6:209–214. https://doi.org/10.1016/j.ccr.2004.09.001

Kadrmas, J.L., and M.C. Beckerle. 2004. The LIM domain: from the cytoskeleton to the nucleus. *Nat. Rev. Mol. Cell Biol.* 5:920–931. https://doi.org/10.1038/nrm1499

Kasof, G.M., L. Goyal, and E. White. 1999. Btf, a novel death-promoting transcriptional repressor that interacts with Bcl-2-related proteins. *Mol. Cell. Biol.* 19:4390–4404. https://doi.org/10.1128/MCB.19.6.4390

Kong, S., S.J. Kim, B. Sandal, S.M. Lee, B. Gao, D.D. Zhang, and D. Fang. 2011. The type III histone deacetylase Sirt1 protein suppresses p300-mediated histone H3 lysine 56 acetylation at Bclaf1 promoter to inhibit T cell activation. *J. Biol. Chem.* 286:16967–16975. https://doi.org/10.1074/jbc.M111.218206

Kwapiszewska, G., M. Wygrecka, L.M. Marsh, S. Schmitt, R. Trösser, J. Wilhelm, K. Helmus, B. Eul, A. Zakrzewicz, H.A. Ghofrani, et al. 2008. Fhl-1, a new key protein in pulmonary hypertension. *Circulation.* 118:1183–1194. https://doi.org/10.1161/CIRCULATIONAHA.107.761916

Lai-Cheong, J.E., M. Parsons, and J.A. McGrath. 2010. The role of kindlins in cell biology and relevance to human disease. *Int. J. Biochem. Cell Biol.* 42:595–603. https://doi.org/10.1016/j.biocel.2009.10.015

Lamy, L., V.N. Ngo, N.C. Emre, A.L. Shaffer III, Y. Yang, E. Tian, V. Nair, M.J. Kruhlak, A. Zingone, O. Landgren, and L.M. Staudt. 2013. Control of autophagic cell death by caspase-10 in multiple myeloma. *Cancer Cell.* 23:435–449. https://doi.org/10.1016/j.ccr.2013.02.017

Lanczky, A., A. Nagy, G. Bottai, G. Munkacsy, L. Paladini, A. Szabo, L. Santarpia, and B. Gyorffy. 2016. miRpower: a web-tool to validate survival-associated miRNAs utilizing expression data from 2,178 breast cancer patients. *Breast Cancer Res. Treat.* 160:439–446.

Larjava, H., E.F. Plow, and C. Wu. 2008. Kindlins: essential regulators of integrin signalling and cell-matrix adhesion. *EMBO Rep.* 9:1203–1208. https://doi.org/10.1038/embor.2008.202

Li, X., Z. Jia, Y. Shen, H. Ichikawa, J. Jarvik, R.G. Nagele, and G.S. Goldberg. 2008. Coordinate suppression of Sdpr and Fhl1 expression in tumors of the breast, kidney, and prostate. *Cancer Sci.* 99:1326–1333. https://doi.org/10.1111/j.1349-7006.2008.00816.x

Lin, J., L. Ding, R. Jin, H. Zhang, L. Cheng, X. Qin, J. Chai, and Q. Ye. 2009. Four and a half LIM domains 1 (FHL1) and receptor interacting protein of 140kDa (RIP140) interact and cooperate in estrogen signaling. *Int. J. Biochem. Cell Biol.* 41:1613–1618. https://doi.org/10.1016/j.biocel.2009.02.007

Liu, Z., D. Lu, X. Wang, J. Wan, C. Liu, and H. Zhang. 2015. Kindlin-2 phosphorylation by Src at Y193 enhances Src activity and is involved in Migfilin recruitment to the focal adhesions. *FEBS Lett.* 589:2001–2010. https://doi.org/10.1016/j.febslet.2015.05.038

Ma, Y.Q., J. Qin, C. Wu, and E.F. Plow. 2008. Kindlin-2 (Mig-2): a co-activator of beta3 integrins. *J. Cell Biol.* 181:439–446. https://doi.org/10.1083/jcb.200710196

McPherson, J.P., H. Sarras, B. Lemmers, L. Tamblyn, E. Migon, E. Matysiak-Zablocki, A. Hakem, S.A. Azami, R. Cardoso, J. Fish, et al. 2009. Essential role for Bclaf1 in lung development and immune system function. *Cell Death Differ.* 16:331–339. https://doi.org/10.1038/cdd.2008.167

Mitra, S.K., and D.D. Schlaepfer. 2006. Integrin-regulated FAK-Src signaling in normal and cancer cells. *Curr. Opin. Cell Biol.* 18:516–523. https://doi.org/10.1016/j.ceb.2006.08.011

Niu, C., C. Liang, J. Guo, L. Cheng, H. Zhang, X. Qin, Q. Zhang, L. Ding, B. Yuan, X. Xu, et al. 2012. Downregulation and growth inhibitory role of FHL1 in lung cancer. *Int. J. Cancer.* 130:2549–2556. https://doi.org/10.1002/ijc.26259

Pascreau, G., F. Eckerdt, A.L. Lewellyn, C. Prigent, and J.L. Maller. 2009. Phosphorylation of p53 is regulated by TPX2-Aurora A in xenopus oocytes. *J. Biol. Chem.* 284:5497–5505. https://doi.org/10.1074/jbc.M805959200

Qu, H., Y. Tu, J.L. Guan, G. Xiao, and C. Wu. 2014. Kindlin-2 tyrosine phosphorylation and interaction with Src serve as a regulatable switch in the integrin outside-in signaling circuit. *J. Biol. Chem.* 289:31001–31013. https://doi.org/10.1074/jbc.M114.580811

Robinson, P.A., S. Brown, M.J. McGrath, I.D. Coghill, R. Gurung, and C.A. Mitchell. 2003. Skeletal muscle LIM protein 1 regulates integrin-mediated myoblast adhesion, spreading, and migration. *Am. J. Physiol. Cell Physiol.* 284:C681–C695. https://doi.org/10.1152/ajpcell.00370.2002

Roskoski, R. Jr. 2015. Src protein-tyrosine kinase structure, mechanism, and small molecule inhibitors. *Pharmacol. Res.* 94:9–25. https://doi.org/10.1016/j.phrs.2015.01.003

Sarras, H., S. Alizadeh Azami, and J.P. McPherson. 2010. In search of a function for BCLAF1. *Sci. World J.* 10:1450–1461. https://doi.org/10.1100/tsw.2010.132

Shao, A.W., H. Sun, Y. Geng, Q. Peng, P. Wang, J. Chen, T. Xiong, R. Cao, and J. Tang. 2016. Bclaf1 is an important NF-κB signaling transducer and C/EBPβ regulator in DNA damage-induced senescence. *Cell Death Differ.* 23:865–875. https://doi.org/10.1038/cdd.2015.150

Shathasivam, T., T. Kislinger, and A.O. Gramolini. 2010. Genes, proteins and complexes: the multifaceted nature of FHL family proteins in diverse tissues. *J. Cell. Mol. Med.* 14:2702–2720. https://doi.org/10.1111/j.1582-4934.2010.01176.x

Shen, Y., Z. Jia, R.G. Nagele, H. Ichikawa, and G.S. Goldberg. 2006. SRC uses Cas to suppress Fhl1 in order to promote nonanchored growth and migration of tumor cells. *Cancer Res.* 66:1543–1552. https://doi.org/10.1158/0008-5472.CAN-05-3152

Tu, Y., S. Wu, X. Shi, K. Chen, and C. Wu. 2003. Migfilin and Mig-2 link focal adhesions to filamin and the actin cytoskeleton and function in cell shape modulation. *Cell.* 113:37–47. https://doi.org/10.1016/S0092-8674(03)00163-6

Veith, C., L.M. Marsh, M. Wygrecka, K. Rutschmann, W. Seeger, N. Weissmann, and G. Kwapiszewska. 2012. Paxillin regulates pulmonary arterial smooth muscle cell function in pulmonary hypertension. *Am. J. Pathol.* 181:1621–1633. https://doi.org/10.1016/j.ajpath.2012.07.026

Wang, X., Z. Yang, H. Zhang, L. Ding, X. Li, C. Zhu, Y. Zheng, and Q. Ye. 2008. The estrogen receptor-interacting protein HPIP increases estrogen-responsive gene expression through activation of MAPK and AKT. *Biochim. Biophys. Acta.* 1783:1220–1228. https://doi.org/10.1016/j.bbamcr.2008.01.026

Wei, X., X. Wang, J. Zhan, Y. Chen, W. Fang, L. Zhang, and H. Zhang. 2017. Smurf1 inhibits integrin activation by controlling Kindlin-2 ubiquitination and degradation. *J. Cell Biol.* 216:1455–1471. https://doi.org/10.1083/jcb.201609073

Willis, T.A., C.L. Wood, J. Hudson, T. Polvikoski, R. Barresi, H. Lochmüller, K. Bushby, and V. Straub. 2016. Muscle hypertrophy as the presenting sign in a patient with a complete FHL1 deletion. *Clin. Genet.* 90:166–170. https://doi.org/10.1111/cge.12695

Xu, X., Z. Fan, C. Liang, L. Li, L. Wang, Y. Liang, J. Wu, S. Chang, Z. Yan, Z. Lv, et al. 2017. A signature motif in LIM proteins mediates binding to checkpoint proteins and increases tumour radiosensitivity. *Nat. Commun.* 8:14059. https://doi.org/10.1038/ncomms14059

Xu, Y., Z. Liu, and K. Guo. 2012. Expression of FHL1 in gastric cancer tissue and its correlation with the invasion and metastasis of gastric cancer. *Mol. Cell. Biochem.* 363:93–99. https://doi.org/10.1007/s11010-011-1161-2

Yeatman, T.J. 2004. A renaissance for SRC. *Nat. Rev. Cancer.* 4:470–480. https://doi.org/10.1038/nrc1366

Zheng, Q., and Y. Zhao. 2007. The diverse biofunctions of LIM domain proteins: determined by subcellular localization and protein-protein interaction. *Biol. Cell.* 99:489–502. https://doi.org/10.1042/BC20060126

Zhou, X., X. Li, Y. Cheng, W. Wu, Z. Xie, Q. Xi, J. Han, G. Wu, J. Fang, and Y. Feng. 2014. BCLAF1 and its splicing regulator SRSF10 regulate the tumorigenic potential of colon cancer cells. *Nat. Commun.* 5:4581. https://doi.org/10.1038/ncomms5581